Identifizierung von Krankheitsvarianten in *CELSR3* und Charakterisierung der embryonalen Funktion von Celsr3 im Zebrafisch

Inaugural-Dissertation

zur Erlangung des Doktorgrades

der Hohen Medizinischen Fakultät

der Rheinischen Friedrich-Wilhelms-Universität

Bonn

Jil Debora Stegmann

aus Bielefeld

2024

Angefertigt mit der Genehmigung
der Medizinischen Fakultät der Universität Bonn

1. Gutachter: Prof. Dr. med. Heiko M. Reutter
2. Gutachter: Prof. Dr. med. Albert J. Becker

Tag der Mündlichen Prüfung: 05.08.2024

Aus dem Eltern-Kind-Zentrum am Universitätsklinikum Bonn
Direktor: Prof. Dr. med. Rainer Ganschow

Inhaltsverzeichnis

Abkürzungsverzeichnis

aa	Amino acid (Aminosäure)
bp	Base pair (Basenpaar)
CADD	Combined Annotation Dependent Depletion (*in silico* Analyseprogramm)
CAKUT	Congenital Anomalies of the Kidney and Urinary Tract (angeborene Anomalien der Nieren und Harnwege)
DNA	Deoxyribonucleic acid (Desoxyribonukleinsäure)
dpf	Days post fertilization (Tage nach der Befruchtung)
KD	*knockdown*
KO	*knockout*
MAF	Minor Allele Frequency (relative Allelhäufigkeit)
MIP	Molecular Inversion Probe (Technologie zur DNA-Sequenzierung)
MO	Morpholino® (Firma: GeneTools, LLC)
NTD	Neural tube defect (Neuralrohrdefekt)
PCP	Planar cell polarity (planare Zellpolarität)
PCR	Polymerase chain reaction (Polymerase-Kettenreaktion)
PolyPhen-2	Polymorphism-Phenotyping v2 (*in silico* Analyseprogramm)
PTU	1-Phenyl-2-Thioharnstoff
RNA	Ribonucleic acid (Ribonukleinsäure)
SB	splice-blocking (Inhibiert das Spleißen)
sgRNA	single-guide RNA (RNA für CRISPR-Cas9 Experimente)

SIFT	Sorting Intolerant From Tolerant (*in silico* Analyseprogramm)
TB	translation-blocking (Inhibiert die Translation)
Tg	transgenic (transgen)
Wt	Wildtyp-Linie im Zebrafisch
Zfl	Zebrafischlarven
ZNS	Zentrales Nervensystem

1. Deutsche Zusammenfassung

1.1 Einleitung

Angeborene Anomalien des zentralen Nervensystems (ZNS) sowie der Nieren und Harnwege (engl. Congenital Anomalies of the Kidney and Urinary Tract, CAKUT) können sowohl isoliert als auch kombiniert mit anderen angeborenen Erkrankungen im Rahmen eines syndromalen Krankheitsbildes auftreten (Colin et al., 2014; Connaughton et al., 2020). Angeborene anatomische oder funktionelle Anomalien des ZNS und der Harnwege können familiär gehäuft auftreten (Colin et al., 2014). Das familiäre Auftreten dieser Anomalien legt nahe, dass genetische Faktoren in der Entstehung der Anomalien eine wichtige Rolle spielen. Eine der häufigsten Formen angeborener Anomalien des ZNS stellen Neuralrohrdefekte (engl. neural tube defects, NTDs) dar, von denen weltweit ca. zwei von 1.000 Neugeborene betroffen sind (Kancherla, 2023). Während der embryologischen Entwicklung können funktionelle Veränderungen verschiedener Mechanismen, wie der planaren Zellpolarität (engl. planar cell polarity, PCP), zu einem unvollständigen Verschluss des Neuralrohres und damit zu Neuralrohrdefekten führen (Greene und Copp, 2014). Durch ein wachsendes Verständnis der embryologischen Entwicklung des ZNS, konnten bereits zahlreiche regulierende genetische und nicht-genetische Faktoren identifiziert werden, wodurch Möglichkeiten der Prävention und Therapie von NTDs entwickelt wurden (Greene und Copp, 2014).

CAKUT umfassen ein breites Spektrum struktureller Anomalien, die auf Defekte in der Morphogenese der Nieren oder Harnwege zurückzuführen sind. Sie gehören zu den häufigsten angeborenen Anomalien und verursachen beinahe 50 % aller chronischen Nierenerkrankungen in den ersten drei Lebensjahrzehnten (Connaughton et al., 2020). Die Prävalenz der CAKUT wird auf 4 - 60 pro 10.000 Geburten geschätzt, wobei die Diagnostik stark von der Untersuchungsmethode, regionalen Einflüssen und dem Schweregrad der Erkrankung abhängt (Murugapoopathy und Gupta, 2020). In vielen Fällen konnten bereits ursächliche genetische Variationen für isolierte oder syndromale CAKUT festgestellt werden (van der Ven et al., 2018). Die Identifizierung potenzieller Kandidatengene für angeborene Anomalien bietet die Möglichkeit der Beratung

betroffener Personen und Familien und stellt das Fundament für die Entwicklung von (pränataler) Diagnostik und Therapiemöglichkeiten.

Als Grundlage für diese Dissertation wurden biallelische Varianten in *CELSR3* bei einem weiblichen Individuum mit bilateraler Hydronephrose, Megaureter, Blasenekstrophie und Tethered-Cord-Syndrom identifiziert (Reutter et al., 2016). Biallelische Varianten betreffen beide Allele eines Gens und können entweder von den Eltern vererbt worden oder neu entstanden sein. *CELSR3* kodiert für einen adhäsiven G-Protein-gekoppelten Rezeptor und ist an der Regulation von PCP sowie der neuronalen und endokrinen Zelldifferenzierung während der embryologischen Entwicklung beteiligt (Wang et al., 2014). Ziel der vorliegenden Dissertation war es bei weiteren Individuen mit Anomalien des ZNS und/oder mit CAKUT Varianten in *CELSR3* zu identifizieren und Celsr3 funktionell zu charakterisieren. Dafür untersuchte ich 734 Individuen mit Hilfe der Molecular Inversion Probe (MIP) Technologie und etablierte internationale Kollaborationen, um weitere Individuen mit Varianten in *CELSR3* zu identifizieren. Zur weiteren Charakterisierung von Celsr3 habe ich Morpholino® *knockdown* (MO-KD) und CRISPR-Cas9 *knockout* (F0-KO) Experimente an Zebrafischlarven (Zfl) verschiedener fluoreszierender Reporterlinien durchgeführt, die spezifisch die neuronale Morphogenese und Nephrogenese zeigen.

Die folgende Originalpublikation stellt die Grundlage der vorliegenden Dissertationsschrift dar:

Stegmann JD, Kalanithy JC, Dworschak GC, Ishorst N, Mingardo E, Lopes FM, Ho YM, Grote P, Lindenberg TT, Yilmaz Ö, Channab K, Seltzsam S, Shril S, Hildebrandt F, Boschann F, Heinen A, Jolly A, Myers K, McBride K, Bekheirnia MR, Bekheirnia N, Scala M, Morleo M, Nigro V, Torella A, Pinelli M, Capra V, Accogli A, Maitz S, Spano A, Olson RJ, Klee EW, Lanpher BC, Jang SS, Chae J-H, Steinbauer P, Rieder D, Janecke AR, Vodopiutz J, Vogel I, Blechingberg J, Cohen JL, Riley K, Klee V, Walsh LE, Begemann M, Elbracht M, Eggermann T, Stoppe A, Stuurman K, van Slegtenhorst M, Barakat TS, Mulhern MS, Sands TT, Cytrynbaum C, Weksberg R, Isidori F, Pippucci T, Severi G, Montanari F, Kruer MC, Bakhtiari S, Darvish H, Reutter H, Hagelueken G, Geyer M, Woolf AS, Posey JE, Lupski JR, Odermatt B, Hilger AC. Bi-allelic variants in

CELSR3 are implicated in central nervous system and urinary tract anomalies. NPJ genomic medicine 2024; 9: 18

1.2 Material und Methoden

Als Grundlage dieser Dissertationsschrift wurden mittels systematischer Exomsequenzierungen biallelische Varianten in *CELSR3* bei einem weiblichen Individuum mit bilateraler Hydronephrose, Megaureter, Blasenekstrophie und Tethered-Cord-Syndrom identifiziert (Reutter et al., 2016). Damit wurde *CELSR3* erstmals als Kandidatengen für CAKUT beschrieben. Um weitere Individuen mit Varianten in *CELSR3* zu identifizieren, führte ich Sequenzierungen von *CELSR3* in 734 Individuen mit Ekstrophien der Harnblase oder anorektalen Malformationen durch (Köllges et al., 2023). Um alle proteinkodierenden Regionen von *CELSR3* zu sequenzieren, habe ich 100 einzelne MIPs mit dem MIPgen Tool entworfen (Boyle et al., 2014). Für eine gleichmäßige Sequenzierung von *CELSR3* erfolgten insgesamt vier Probe-Sequenzierungen mit dem MiSeq® (Illumina, Reagent Kit v2) zur Anpassung der einzelnen MIPs, bevor alle 734 Proben mit Desoxyribonukleinsäure (engl. Deoxyribonucleic acid, DNA) der betroffenen Individuen mit dem NovaSeq 6000® (Illumina, XP-Workflow Reagent Kit v1.5) in der Next Generation Sequencing Core Facility der Universität Bonn sequenziert werden konnten. Alle identifizierten Varianten filterte ich hinsichtlich der Sequenzierungsqualität und der relativen Allelhäufigkeit (engl. Minor Allele Frequency, MAF) mit einer MAF ≤ 0,0001 bei gnomAD v3.1, um die Wahrscheinlichkeit für das Vorkommen der Variante in der gesunden Allgemeinbevölkerung zu minimieren. Mit Sanger-Sequenzierungen validierte ich die einzelnen Varianten und deren Vererbungsmuster, sofern elterliche DNA zur Verfügung stand.

Ergänzend zu den MIPs Studien konnte ich über GeneMatcher internationale Kollaborationen aufbauen und weitere zwölf Individuen mit Anomalien des ZNS, CAKUT oder kombinierten Erkrankungen identifizieren und meiner wissenschaftlichen Arbeit zuführen (Sobreira et al., 2015). Die Patientenrekrutierung und Durchführung genetischer Studien wurde von den Ethikkommissionen der jeweiligen beteiligten

Institutionen genehmigt. Bei allen eingeschlossenen Individuen wurden biallelische Varianten in *CELSR3* mit einer MAF ≤ 0,0001 bei gnomAD v3.1 identifiziert und mittels Sanger-Sequenzierung bestätigt. Anhand computerbasierter *in silico* Simulationen analysierte ich alle inkludierten Varianten hinsichtlich ihrer Pathogenität auf Basis der einzelnen Veränderungen der Nukleotide und der daraus kodierenden CELSR3 Proteinregionen. Dafür verwendete ich die folgenden online verfügbaren Programme: Combined Annotation Dependent Depletion GRCh38-v1.6 (CADD), Polymorphism-Phenotyping v2 (PolyPhen-2), Sorting Intolerant From Tolerant (SIFT), MetaDome Version 1.0.1 und ConSurf (Rentzsch et al., 2019; Adzhubei et al., 2010; Sim et al., 2012; Wiel et al., 2019; Ben Chorin et al., 2020; Goldenberg et al., 2009). Ergänzend dazu hat im Rahmen dieser Publikation das Institut für strukturelle Biologie der Universität Bonn mittels AlphaFold ein computerbasiertes 3D Modell des CELSR3 Proteins entwickelt (Jumper et al., 2021). Anhand dessen konnten wir einen Großteil der CELSR3 Proteinstruktur akkurat nachvollziehen und den Effekt der identifizierten Varianten für die 3D Proteinstruktur bildlich darstellen.

Um *CELSR3* als potenzielles Kandidatengen für CAKUT zu charakterisieren, führten unsere Kooperationspartner der Universität Manchester unter der Leitung von Prof. Dr. Adrian Woolf Expressionsstudien mittels eines polyklonalen Anti-CELSR3 Antikörpers (ab189012 von Abcam) an den Nieren und Harnwegen im Gewebe eines sieben-, zehn- und zwölfwöchigen humanen Embryos durch. Das Embryonalgewebe wurde nach der Zustimmung der Mutter und Genehmigung der entsprechenden Ethikkommission (REC18/NE/0290) entnommen und für Forschungszwecke verwendet (Lopes et al., 2019). Zusätzlich konnte ich, basierend auf den Arbeiten von Dr. Phillip Grote (Georg-Speyer-Haus, Frankfurt am Main) und Dr. Enrico Mingardo (Universität Bonn), die Expression von *CELSR3*/*Celsr3* Ribonukleinsäure (engl. Ribonucleic acid, RNA) im Harnblasengewebe von sieben- bis neunwöchigen humanen Embryos und embryonalen Mäusen E10.5 – E12.5 quantifizieren (GEO accession ID: GSE190641, Mingardo et al., 2022).

Um die Rolle von *CELSR3* während der Entwicklung des Harntraktes und des ZNS weiter zu charakterisieren, führte ich in Kooperation mit der Arbeitsgruppe von Prof. Dr. Benjamin Odermatt am Anatomischen Institut in Bonn Studien in Zebrafischlarven (Zfl)

durch. Der Zebrafisch eignet sich aufgrund seiner Transparenz im Larvenstadium und seiner Entwicklung außerhalb des Uterus besonders gut als Vertebraten-Modellorganismus für Entwicklungsstudien und hat sich in den letzten Jahrzehnten als attraktiver Modellorganismus zur Untersuchung der embryonalen Neurogenese erwiesen (Schmidt et al., 2013). Im Gegensatz zu Säugetieren weist der Zebrafisch ein viel größeres Proliferationspotenzial mit einer verstärkten neurogenen Aktivität auf, wodurch sich die Neurogenese sehr gut in Zfl untersuchen lässt (Schmidt et al., 2013). Die Entwicklung des Harntraktes erfolgt im Zebrafisch vergleichbar zu der humanen Nephrogenese durch ein komplexes Zusammenwirken zellulärer Migration, Epithelialisierung und dem Einwirken multipler molekulargenetischer Faktoren (Naylor et al., 2017). Anders als beim Menschen, bei dem die Niere im Durchschnitt eine Million Funktionssysteme aus Glomeruli und Tubuli (Nephrone) beinhaltet, besteht die Niere in der Zebrafischlarve nur aus einer Vorniere (Pronephros) mit einem singulären Glomerulus und zwei daraus ableitenden Tubulussystemen (Naylor et al., 2017). Sie stellt damit eine vereinfachte Version der menschlichen Niere dar und eignet sich dadurch besonders gut zur Charakterisierung von Anomalien der sich entwickelnden Nieren und Harnwege.

Die Haltung der Zebrafische und die Versuchsaufbauten entsprechen den europäischen Tierversuchsrichtlinien. Zfl der Wildtyp-Linie (Wt), sowie transgene (engl. transgenic, Tg) Fischlinien *Tg(-3.1ngn1:GFP)*, *Tg(wt1b:EGFP)* und *Tg(HGj4A)* zur Charakterisierung der Entwicklung des ZNS, des Pronephros und der Kloake wurden durch natürliche Laichung gewonnen und bei standardisierten Temperatur- und Lichtbedingungen aufgezogen. Alle Experimente wurden in der Zebrafish Core Facility der Medizinischen Fakultät der Universität Bonn an Zfl in einem Alter von ein bis fünf Tagen nach der Befruchtung (engl. days post fertilization, dpf) durchgeführt. Um die phänotypischen Auswirkungen eines *knockdowns* (KD) von Celsr3 im Zebrafisch zu untersuchen, habe ich spezifische Antisense-Morpholinos® (MOs) gegen *celsr3* mit der Software von GeneTools LLC entworfen, die entweder an die transkribierte mRNA am Startcodon binden und somit die Translation inhibieren (engl. translation-blocking MO, TB-MO) oder an die Exon-Intron-Grenzen binden und somit das Spleißen inhibieren (engl. splice-blocking MO, SB-MO), was beides zu einer verminderten Proteinsynthese führt. Zur Identifizierung des Startcodons habe ich eine computerbasierte Sequenzanalyse der

Celsr3-Proteine verschiedener Spezies mittels SerialCloner 2.6.1 und eine experimentelle Analyse der Region des Startcodons durchgeführt, da *celsr3* in Zfl mit vier teilweise überlappenden Transkripten beschrieben wird (Ensembl Version 107; Cunningham et al., 2022). Dafür extrahierte ich RNA aus 35 Zfl mit TRIzol™-Reagenz (Thermo Fisher Scientific, Katalog-Nr. 15596026) und führte Reverse-Transkriptase-Polymerase-Kettenreaktionen (engl. polymerase chain reaction, PCR) mit dem ProtoScript® II First Strand cDNA Synthesis Kit (New England BioLabs GmbH, Katalog-Nr. E6560) sowie cDNA-Amplifikationen mit selbst designten Primerpaaren durch. In ein- bis zweizelligen Zf-Embryonen führte ich anschließend MO-Mikroinjektionen mit ~ 4,5 ng (1,8 nl / Embryo) *celsr3* TB-MO-201, *celsr3* TB-MO-204 oder dem Standard-Kontroll-MO bzw. mit ~ 5,9 ng *celsr3* SB-MO (1,8 nl / Embryo) durch. Für die Injektionen untersuchte ich in separaten Versuchsreihen Konzentrationen zwischen ~ 3,7 – 7,4 ng MO, um dosisabhängige Effekte zu identifizieren und toxische Konzentrationen im weiteren Verlauf der Experimente zu vermeiden.

Um die Spezifität der MO-KDs zu überprüfen, etablierte ich sogenannte *CELSR3* mRNA Rescue Experimente. Dabei „rettet“ humane Wt *CELSR3* mRNA den Phänotyp (Rescue), sofern der verwendete MO mit einer für die Zebrafisch mRNA spezifischen Erkennungssequenz nicht an die humane *CELSR3* mRNA binden kann. Mit einem humanen *CELSR3* cDNA ORF-Klon (GenScript, OHu18524) und Reagenzien von Thermo Fisher Scientific (Katalog Nr. AMB13455 und AM1350) habe ich die in vitro Transkription und Polyadenylierung der Wt *CELSR3* mRNA durchgeführt. Für die Rescue Experimente co-injizierte ich ~ 70 pg humane Wt *CELSR3* polyA-mRNA mit *celsr3* TB-MO-204 und charakterisierte die Zfl phänotypisch zwischen 1 – 5 dpf. Anhand von separaten Versuchsreihen untersuchte ich vorab dosisabhängige Effekte mit Injektionen verschiedener Konzentrationen zwischen 20 – 100 pg / nl *CELSR3* polyA-mRNA, um toxische Konzentrationen zu vermeiden.

Ergänzend dazu führte ich mit Unterstützung von Dr. Nina Ishorst *celsr3* CRISPR–Cas9 F0 *knockout* (F0-KO) Experimente durch. Dafür entwarfen wir sechs sgRNAs (engl. single-guide RNA) spezifisch für die Sequenz von *celsr3* in Zfl und drei (nicht bindende) Kontroll sgRNAs mittels der Website CRISPRscan (Moreno-Mateos et al., 2015). Komplementäre Abschnitte der sgRNAs binden an Sequenzen der genomischen DNA,

welche von Cas9 im Doppelstrang geschnitten und mittels DNA-Reparaturmechanismen wieder zusammengefügt werden. Hierbei entstehen Insertionen und/oder Deletionen, die schließlich bei > 99 % der injizierten Zfl zu einem fehlerhaft translatierten Protein führen (Jobst-Schwan et al., 2018). Die Reagenzien für die CRISPR-Cas9 F0-KO Experimente nutzten wir von Integrated DNA Technologies, Inc. (Essner, 2016). Wir injizierten ~ 1,8 nl der *celsr3* CRISPR-Cas9 KO Lösung oder der Kontroll-Lösung in den Dotter von ein- bis zweizelligen Zf-Embryonen und charakterisierten die Zfl zwischen 1 – 5 dpf. Mittels PCR untersuchten wir anschließend den Effekt der CRISPR Cas9 F0-KO Experimente auf die genomische Region von *celsr3*.

Zur Phänotypisierung der Zfl führte ich die oben genannten Versuchsreihen sowohl an Wt Zfl als auch an transgenen fluoreszierenden Reporter-Zfl *Tg(-3.1ngn1:GFP)*, *Tg(wt1b:EGFP)* und *Tg(HGj4A)* durch und beobachtete die Zfl bis zu 5 dpf. Für die *in vivo* Visualisierung und Fotodokumentation nutzte ich ein ZEISS Axio V16 Multi-Zoom Fluoreszenzmikroskop mit der ZEN 2.3 Software und ein konfokales Laser-Scanning Mikroskop Nikon A1R HD25 ECLIPSE Ti2E mit der NIS-Elements 5.21.02 Software. Für eine bessere Vergleichbarkeit der Zfl habe ich die Zfl zu dem Zeitpunkt der Phänotypisierung mit 0,03 % Tricain anästhesiert und in 1,25 % niedrigschmelzender Agarose fixiert. Alle Experimente wiederholte ich mehrmals unabhängig voneinander und die drei zuverlässigsten Versuchsreihen mit durchgehend guter Beurteilung der Larven an allen fünf Beobachtungstagen wurden in das Manuskript aufgenommen. Die statistische Auswertung führte ich mit GraphPad Prism Software Version 9.0.0 durch. Die statistischen Analysen umfassten Kaplan-Meier-Überlebenskurven und ANOVA-Tests, wobei eine statistische Signifikanz bei einem p-Wert < 0,05 (*) angenommen wurde.

1.3 Ergebnisse

Mittels DNA-Sequenzierungen von 734 Individuen mit Ekstrophien der Harnblase oder anorektalen Malformationen wurden insgesamt 564 Varianten in *CELSR3* detektiert. Davon erfüllten 15 Varianten (14 Missense-Varianten und eine *in-frame*-Deletion) in 16 unabhängigen Individuen die zuvor definierten Filterkriterien hinsichtlich der

Sequenzierungsqualität und des seltenen Auftretens in der gesunden Allgemeinbevölkerung (Tab. 1). In computerbasierten Vorhersageprogrammen wurden 10 der 15 Varianten als potenziell krankheitsverursachend charakterisiert. In den daran anschließenden Sanger-Sequenzierungen wurden alle identifizierten Varianten als heterozygot bestätigt, also nur eines der beiden Allele betreffend (monoallelisch). Bei 9 von 16 Individuen konnte eine elterliche Vererbung validiert werden, wobei die Eltern als gesund beschrieben wurden. Die Variante c.G6349A, p.(V2117M) wurde in zwei nicht-verwandten Individuen mit anorektalen Malformationen identifiziert (Individuum 9 und 14), wovon bei Individuum 9 ebenfalls die gesunde Mutter die Variante trägt. Unter Berücksichtigung aller Ergebnisse wurden alle heterozygoten Varianten, die von gesunden Elternteilen vererbt wurden, als wahrscheinlich nicht-krankheitsverursachend bewertet. Folglich verblieben sieben heterozygote Varianten in sieben nicht-verwandten Individuen (Individuum 10 – 16) von unklarer Signifikanz aufgrund unvollständiger elterlicher DNA.

Tab. 1: Daten von Individuen mit monoallelischen Varianten in *CELSR3*. Übersicht zu klinischen und molekularen Daten von 16 Individuen mit monoallelischen Varianten in *CELSR3*, identifiziert durch die *Molecular Inversion Probe* (MIP) Technologie und bestätigt durch Sanger-Sequenzierungen inklusive Analyse des Vererbungsmusters, sofern elterliche DNA zur Verfügung stand. *Nr* Nummer, *VACTERL* Assoziation angeborener Fehlbildungen (vertebral defects, anal atresia, cardiac defects, tracheo-esophageal fistula, renal anomalies, limb abnormalities), *bds* beidseitig, *CADD* CADD-Score (Combined Annotation Dependent Depletion GRCh37-v1.6), *P* PolyPhen-2 (Polymorphism-Phenotyping v2, *1* benign, *2* possibly damaging, *3* probably damaging), *S* SIFT (Sorting Intolerant From Tolerant, *T* tolerated, *D* deleterious), *V* Vater, *M* Mutter, *Wt* Wildtyp, *X* keine Daten verfügbar.

Nr.	**Phänotyp**	***CELSR3***	**CADD; P; S**	**Kommentar**
1	Blasenekstrophie, Hernien bilateral	c.G9194A, p.(R3065H)	29,9; 3; D	V heterozygot
2	Blasenekstrophie, Hernien bilateral	c.9520_9521del, p.(L3174fs22*)	X	V heterozygot
3	Blasenekstrophie, Hernien bilateral, Hämangiom	c.C9265G, p.(P3089A)	16,84; 1; T	M heterozygot
4	Blasenekstrophie	c.T4735G, p.(S1579A)	28,5; 3; D	M heterozygot
5	Blasenekstrophie	c.C1094T, p.(A365V)	23; 1; T	M heterozygot
6	Blasenekstrophie	c.C4958T, p.(A1653V)	26,5; 3; D	M heterozygot
7	Anorektale Malformation mit vestibulärer Fistel, Ösophagusatresie	c.C9380T, p.(P3127L)	23,3; 1; T	V heterozygot
8	Anorektale Malformation im Sinne einer perinealen Fistel, Hymenalatresie, Doppelniere links, Beinverkürzung links, bikuspide Aortenklappe	c.C7019G, p.(A2340G)	15,91; 1; T	M heterozygot
9	Anorektale Malformation im Sinne einer perinealen Fistel, leichte kraniozerebrale Fehlbildung	c.G6349A, p.(V2117M)	27,5; 2; D	M heterozygot
10	Blasenekstrophie	c.C9860T, p.(T3287M)	24,7; 2; D	Eltern nicht sequenziert
11	Blasenekstrophie	c.C6523G, p.(L2175V)	25,3; 3; D	Eltern nicht sequenziert
12	Blasenekstrophie	c.C2962T, p.(R988W)	27,5; 3; D	Eltern nicht sequenziert
13	Blasenekstrophie	c.G1880A, p.(R627Q)	26,5; 3; D	V nicht sequenziert, M Wt
14	Anorektale Malformation im Sinne einer perinealen Fistel, VACTERL, Entwicklungsverzögerung	c.G6349A, p.(V2117M)	27,5; 2; D	V nicht sequenziert, M Wt
15	Rektourethrale Fistel, Ösophagusatresie	c.G7657A, p.(A2553T)	23,2; 2; D	V nicht sequenziert, M Wt
16	VACTERL, rektovesikale Fistel, Hüftluxation bds, Meningomyelozele, Nierenagenesie rechts	c.G9245A, p.(R3082H)	22,1; 1; D	V nicht sequenziert, M Wt

Zusätzlich konnten durch internationale Kollaborationen zwölf Individuen aus elf unabhängigen Familien mit biallelischen Varianten in *CELSR3* ermittelt werden, darunter sieben Individuen mit ZNS-Anomalien, drei Individuen mit kombinierten ZNS-Anomalien und CAKUT und zwei Individuen mit CAKUT. Individuen mit ZNS-Anomalien zeigten Auffälligkeit in Form von Intelligenzminderung und/oder Entwicklungsverzögerung, muskulärer Hypotonie, Krampfanfällen, Hirnfehlbildungen, NTDs, Makro- oder Mikrozephalie. Individuen mit CAKUT zeigten Duplikationen der Harnsysteme, ektope Nieren, multizystische dysplastische Nieren, vesikoureteralen Reflux, Hydronephrose, obstruktive Uropathien oder eine unregelmäßige Blasenwand. Anhand von Vorhersageprogrammen wurden 13 der 16 Varianten in *CELSR3* als potenziell krankheitsverursachend charakterisiert. Alle Varianten außer c.8480C>A haben einen CADD-Score > 22 und alle Varianten außer c.3142C>T befinden sich in evolutionär hoch konservierten Regionen. Die 3D-Modellierungen von CELSR3 zeigen detailliert die einzelnen Proteindomänen, wovon 2540 Aminosäuren (engl. amino acids, aa) extrazellulär (N-Terminal), 233 aa die Zellmembran überspannend und 522 aa intrazellulär (C-Terminal) lokalisiert sind. Zusätzlich konnte anhand des Modells der Effekt der einzelnen Varianten für die 3D Struktur des Proteins beurteilt und eine phänotypische Verteilung der Varianten festgestellt werden. Sieben von zehn Varianten der Individuen mit ZNS-Anomalien befinden sich nahe der Zellmembran oder intrazellulär (C-Terminal). Alle Varianten, die bei Individuen mit CAKUT identifiziert wurden, befinden sich in extrazellulären Domänen von CELSR3.

Die Expression von Celsr3 im ZNS von Mäusen wird in der Literatur bereits umfassend beschrieben (Shima et al., 2002; Zhou et al., 2008). Durch antikörperbasierte Expressionsanalysen in Gewebsschnitten eines sieben-, zehn- und zwölfwöchigen menschlichen Embryos konnten wir ergänzend dazu CELSR3 in den embryonalen Vorläufern der Nieren und Harnwege detektieren. Zusätzlich zeigten *CELSR3* mRNA Expressionsdaten die Expression von *CELSR3* in embryonalem Harnblasengewebe von sieben- bis neunwöchigen menschlichen Embryonen und embryonalen Mäusen (E10,5 – E12,5).

Um die Rolle von *CELSR3* in der Entwicklung des ZNS und der Harnwege genauer zu charakterisieren, führte ich KD- und KO-Experimente in sich entwickelnden Zfl durch. In

bisherigen öffentlichen Datenbanken wird *celsr3* im Zf mit vier teilweise überlappenden Transkripten beschrieben und ohne eine Sequenz, die als Startcodon fungieren könnte (Ensembl Version 107; Cunningham et al., 2022). In den meisten Fällen wird die Proteinsynthese durch das Startcodon des RNA-Basentripletts AUG initiiert, das für die Aminosäure Methionin kodiert (Drabkin und RajBhandary, 1998). Um ergänzend zu den öffentlichen Datenbanken die transkribierte Region von *celsr3* besser nachvollziehen zu können, führte ich initial PCR-Amplifikationen von Zf-cDNA durch. Dabei konnte am 5´Ende von *celsr3* eine zusätzliche Region von 2138 Basenpaaren (engl. base pair, bp) detektiert und das wahrscheinlichste Startcodon durch den Vergleich der Proteinsequenzen zu anderen Spezies und einer starken Übereinstimmung mit der Kozak-Sequenz identifiziert werden. Die Kozak-Sequenz ist dafür bekannt, dass sie in Eukaryonten mit natürlichen Varianten als Initiationsstelle der Translation vorkommt (Grzegorski et al., 2014). Auf dieser Basis konnte ich einen MO-KD von Celsr3 in Zfl etablieren. Celsr3 KD führte zum Zeitpunkt von zwei dpf bei 42 % der SB-MO-Zfl und 83 % der TB-MO Zfl zu einem übereinstimmenden Phänotyp, welcher sich mit einer veränderten Konfiguration des kaudalen Endes der Zfl darstellte, teilweise in Kombination mit einer Unterbrechung des neuronalen oder muskuloskelettalen Gewebes. Dieser Phänotyp war in beiden MO-Gruppen signifikant ausgeprägt im Vergleich zu der MO-Kontrollgruppe, wo 2 % der Zfl kaudale Veränderungen zeigten. Mit transgenen *Tg(-3.1ngn1:GFP)* Zfl konnte bei drei dpf eine veränderte Anordnung neuronaler Vorläuferzellen und ein verringertes axonales Wachstum in Celsr3 MO-KD Zfl festgestellt werden. Mit transgenen *Tg(wt1b:EGFP)* Zfl wurde die strukturelle Entwicklung des Pronephros bei drei dpf untersucht und eine signifikant häufigere Dilatation des Glomerulus in Celsr3 MO-KD Zfl beobachtet. Zu der Überprüfung, dass die beobachteten Phänotypen auf eine Reduktion des Celsr3 Proteins in Zfl zurückzuführen sind, etablierte ich mRNA Rescue Experimente durch eine co-Injektion von *celsr3* TB-MO und humaner Wt *CELSR3* polyA-mRNA. Dies führte zu einer signifikanten Reduktion des Phänotyps sowohl in Wt Zfl als auch in den Reporterlinien *Tg(-3.1ngn1:GFP)* und *Tg(wt1b:EGFP)* im Vergleich zu den MO-KD Zfl. Zusätzlich konnten in *celsr3* CRISPR Cas9 F0-KO Zfl vergleichbare kaudale Veränderungen und eine erhöhte Mortalität festgestellt werden. In Wt Zfl zeigten 63 % der *celsr3* CRISPR

Cas9 F0-KO Zfl eine kaudale Veränderung, was signifikant erhöht war im Vergleich zu 2 % in der CRISPR-Kontrollgruppe.

In transgenen *Tg(HGj4A)* Zfl ergänzte ich die bisherige Phänotypisierung durch eine Beobachtung der sich entwickelnden unteren Harnwege und der Kloake. Gelegentlich konnte bei *Tg(HGj4A)* Zfl nach fünf dpf ein Phänotyp beobachtet werden, welcher sich in einer Erweiterung zwischen dem pronephrischen Gang (engl. ductus) und dem Enddarm vor der Fusion in der Kloake zeigte (Abb. 1). In der statistischen Auswertung war dieser kloakale Phänotyp jedoch nicht signifikant im Vergleich zu der Kontrollgruppe.

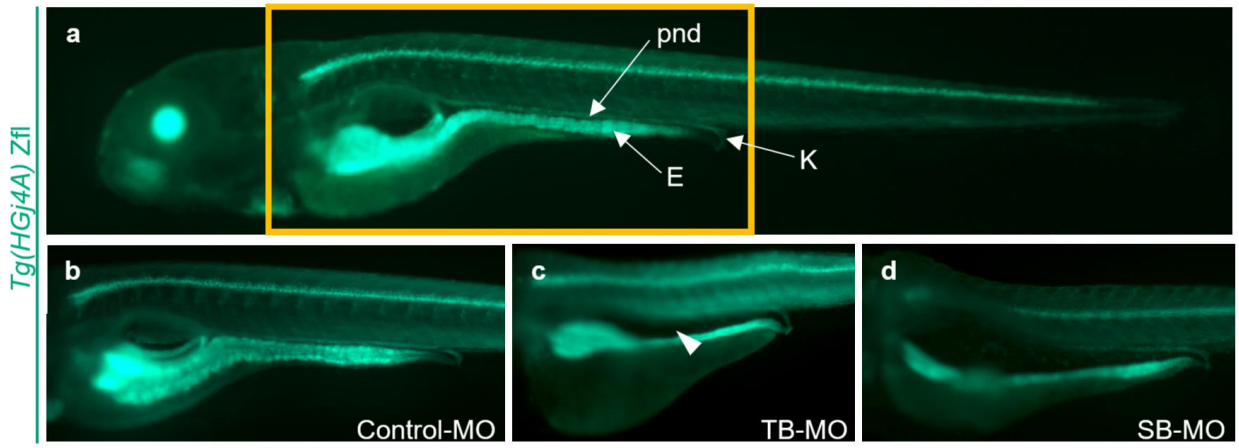

Abb. 1: Vereinzelte kloakale Veränderungen in Celsr3 knockdown Zebrafischlarven. Laterale Ansicht von *Tg(HGj4A)* Zebrafischlarven (Zfl) fünf Tage nach der Befruchtung, behandelt mit 1-Phenyl-2-Thioharnstoff (PTU) zur Vermeidung von Pigmentierung der Zfl. *In vivo* Visualisierung der Zfl mit einem ZEISS Axio V16 Multi-Zoom Mikroskop mit der ZEN 2.3 Software. **a** Übersichtsdarstellung einer *Tg(HGj4A)* Zfl in lateraler Ansicht. *pnd* pronephrischer Gang, *E* Enddarm, *K* Kloake. **b – d** Darstellung ausgewählter Zfl, welche entweder mit Kontroll-Morpholino® (Control-MO), einem die Translation von *celsr3* blockierenden MO (TB-MO) oder einem das Spleißen von *celsr3* inhibierenden MO (SB-MO) injiziert wurden. Gelegentlich kann bei MO-injizierten Zfl ein vergrößerter Raum zwischen dem pronephrischen Gang und dem Enddarm vor der Fusion in der Kloake beobachtet werden (weiße Pfeilspitze). Dies könnte möglicherweise durch ein Ödem oder eine anatomische kloakale Blockade verursacht werden. Dieser Phänotyp zeigte sich nur bei vereinzelten Zfl und nicht signifikant häufiger im Vergleich zu der Kontrollgruppe.

1.4 Diskussion

Angeborene Anomalien können sehr heterogen auftreten, entweder in isolierten Ausprägungsformen innerhalb eines Organsystems oder als Teil eines syndromalen

Krankheitsbildes. In vorherigen Studien wurden seltene monoallelische Varianten in *CELSR3* mit NTDs, Fieberkrämpfen und dem Tourette-Syndrom assoziiert (Chen et al., 2018; Li et al., 2022; Wang et al., 2018). Die im Rahmen dieser Dissertation detektierten monoallelischen Varianten in *CELSR3* konnten auch bei vermeintlich gesunden Individuen festgestellt werden. Es besteht die Möglichkeit, dass zu dem Zeitpunkt der Phänotypisierung milde Ausprägungsformen unentdeckt geblieben sind oder eine pathogene Variante ohne phänotypische Ausprägung bleibt. Dieses Phänomen wird als unvollständige Penetranz bezeichnet und wurde bereits in anderen Familien mit CAKUT und ZNS-Anomalien beobachtet (Cooper et al., 2013; Vivante et al., 2014; Arlt et al., 2022). Penetranz kann durch verschiedene Faktoren wie Geschlecht, Epigenetik, Umweltfaktoren und zusätzlichen Varianten in anderen Genen beeinflusst werden (Cooper et al., 2013). Insgesamt deuten die Ergebnisse der multiplex DNA-Sequenzierungen jedoch darauf hin, dass *CELSR3* als ein rezessives Krankheitsgen untersucht und seltene biallelische Varianten in *CELSR3* im Kontext angeborener ZNS-Anomalien und CAKUT in Betracht gezogen werden sollten.

Für die Identifizierung möglichst vieler Individuen mit seltenen oder nicht vorbeschriebenen biallelischen Varianten in *CELSR3* ist eine internationale Zusammenarbeit erforderlich. Im Rahmen dieser Dissertation konnten bei zwölf Individuen in elf unabhängigen Familien mit einem phänotypischen Kontinuum aus ZNS-Anomalien und CAKUT potenziell krankheitsverursachende Varianten in *CELSR3* analysiert werden. Bei der Auswahl der Individuen wurden strenge Filterkriterien angewendet, um die Wahrscheinlichkeit zufälliger Korrelationen zwischen Varianten in *CELSR3* und Erkrankungen zu minimieren. Dadurch ist die Anzahl der identifizierten Individuen relativ klein, bietet aber dennoch ein solides Fundament für die Charakterisierung eines seltenen Krankheitsbildes. In zukünftigen Studien sollten systematisch größere Kohorten an entsprechenden Zentren untersucht werden, um die Beteiligung von biallelischen Varianten in *CELSR3* im Zusammenhang mit seltenen Erkrankungen noch detaillierter beobachten zu können.

In syndromalen Erkrankungen sind häufig verschiedene Organsysteme in unterschiedlichem Ausmaß klinisch betroffen, wie zum Beispiel beim CHARGE-Syndrom, wo verschiedene angeborene Anomalien isoliert oder in unterschiedlichen

Kombinationen auftreten können (Hsu et al., 2014). Die im Rahmen dieser Dissertation identifizierten Individuen mit biallelischen Varianten in *CELSR3* präsentierten variable phänotypische Ausprägungen im ZNS und der Harnwege. In der Literatur wird verdeutlicht, dass CELSR3 bei neuronaler Migration, PCP und weiteren regulatorischen Prozessen beteiligt ist, welche bereits in frühen Stadien der embryonalen Entwicklung eine Rolle spielen (Wang et al., 2014). Je nach Beeinträchtigung der CELSR3-Proteinfunktion könnte dies zur phänotypischen Variabilität beitragen.

Zusätzlich wurden in dieser Dissertation vergleichbare Phänotypen in Celsr3 MO-KD und *celsr3* CRISPR-Cas9 F0-KO Zfl beobachtet, einschließlich verringertem axonalen Wachstum und strukturellen Veränderungen des Pronephros. Diese Phänotypen traten signifikant häufiger in den KD und F0-KO Zfl auf, jedoch auch innerhalb der Injektionsgruppe in verschiedenen Ausprägungsformen. Anhand der Rescue-Experimente konnte mit humaner *CELSR3* polyA-mRNA das Auftreten des Phänotyps minimiert und damit nachgewiesen werden, dass der spezifische MO-KD von Celsr3 eine entscheidende Rolle in der Pathogenese spielt. Gleichzeitig bestätigten die Rescue Experimente die hohe funktionelle Übereinstimmung zwischen dem humanen *CELSR3* zu dem orthologen *celsr3* im Zebrafisch. Dadurch konnte der Zebrafisch erneut als Modellorganismus zur funktionellen Charakterisierung von *celsr3* bekräftigt werden. Da einige der identifizierten Individuen auch Anomalien der unteren Harnwege oder anorektale Malformationen zeigten, wurden ergänzende MO-KD Experimente mit transgenen *Tg(HGj4A)* Reporter-Zfl durchgeführt. Die vereinzelten kloakalen Veränderungen könnten möglicherweise auf ein Ödem oder eine anatomische kloakale Obstruktion zurückzuführen sein, vergleichbar mit den Individuen mit Hydronephrose und anderen Urintransportstörungen oder anorektalen Malformationen (Abb. 1). Da dieser Phänotyp in den untersuchten Zfl jedoch nicht statistisch signifikant zu beobachten war und nur eine Minderheit der Individuen mit biallelischen Varianten in *CELSR3* (3 der 12 Individuen) Phänotypen aufweisen, die den unteren Harntrakt oder den Enddarm betreffen, kann *CELSR3* zum aktuellen Zeitpunkt nicht als krankheitsverursachendes Gen für kloakale Anomalien bestätigt werden.

Insgesamt bekräftigen die durchgeführten Experimente in Zfl die entscheidende Rolle von Celsr3 in der embryonalen Entwicklung neuronaler und nephrologischer Systeme

und tragen maßgeblich zum Verständnis von *CELSR3* als Krankheitsgen für angeborene Anomalien des ZNS und der Harnwege in variablen Ausprägungsformen bei. Limitierend bleibt jedoch die Unsicherheit über die Funktion der jeweiligen *CELSR3* Varianten bei der Krankheitsentstehung. In zukünftigen Experimenten sollten ergänzende Testungen der *CELSR3* Varianten in funktionellen Studien und zellulären Modellen erfolgen, um die Pathogenität einzelner Varianten genauer zu verstehen.

1.5 Zusammenfassung

Die Ätiologie angeborener Anomalien ist multifaktoriell und wird sowohl durch Umweltfaktoren als auch komplexe genetische Faktoren beeinflusst (Corsello und Giuffrè, 2012). Im Rahmen dieser Dissertation konnten, basierend auf früheren Studien und den durch GeneMatcher etablierten Kollaborationen, zwölf Individuen aus elf unabhängigen Familien hinsichtlich potenziell krankheitsverursachender, biallelischer Varianten in *CELSR3* analysiert werden (Reutter et al., 2016; Sobreira et al., 2015). Die betroffenen Individuen zeigten einen Phänotyp innerhalb eines Kontinuums von Anomalien des zentralen Nervensystems (ZNS) und der Harnwege. *CELSR3* kodiert für einen adhäsiven G-Protein-gekoppelten Rezeptor und ist an vielen embryologischen Prozessen beteiligt, inklusive der Regulierung planarer Zellpolarität und der neuronalen und endokrinen Zelldifferenzierung (Wang et al., 2014). Um die Rolle von CELSR3 im Zusammenhang mit seltenen angeborenen Erkrankungen weiter zu untersuchen, habe ich im Rahmen dieser Dissertation DNA-Sequenzierungen an insgesamt 734 Individuen mit Ekstrophien der Harnblase oder anorektalen Malformationen durchgeführt und dabei sieben nicht-verwandte Individuen mit heterozygoten Varianten in *CELSR3* unklarer klinischer Signifikanz identifiziert (Tab. 1). Zusätzlich publizierten wir im Rahmen dieser Dissertation detaillierte 3D Modellierungen des CELSR3 Proteins inklusive der möglichen Effekte verschiedener *CELSR3* Varianten, Expressionsdaten embryonaler und fetaler Gewebe der Harnwege und *in vivo* Studien in Zebrafischlarven. In fluoreszierenden Reporterlinien, welche spezifisch für das neuronale und nephrologische System in Zfl sind, konnte ich durch Morpholino® *knockdown*, CRISPR-Cas9 F0-*knockout* und Rescue-Experimente die Funktion von Celsr3 während der frühen embryonalen Entwicklung des ZNS und der Harnwege genauer charakterisieren.

Anhand dieser molekulargenetischen und funktionellen Studien konnte *CELSR3* als ein wahrscheinliches Krankheitsgen für variable Ausprägungsformen angeborener Erkrankungen des ZNS und der Harnwege identifiziert werden.

1.6 Literaturverzeichnis der deutschen Zusammenfassung

Adzhubei IA, Schmidt S, Peshkin L, Ramensky VE, Gerasimova A, Bork P, Kondrashov AS, Sunyaev SR. A method and server for predicting damaging missense mutations. Nature methods 2010; 7: 248–249

Arlt A, Kohlschmidt N, Hentschel A, Bartels E, Groß C, Töpf A, Edem P, Szabo N, Sickmann A, Meyer N, Schara-Schmidt U, Lau J, Lochmüller H, Horvath R, Oktay Y, Roos A, Hiz S. Novel insights into PORCN mutations, associated phenotypes and pathophysiological aspects. Orphanet journal of rare diseases 2022; 17: 29

Ben Chorin A, Masrati G, Kessel A, Narunsky A, Sprinzak J, Lahav S, Ashkenazy H, Ben-Tal N. ConSurf-DB: An accessible repository for the evolutionary conservation patterns of the majority of PDB proteins. Protein science : a publication of the Protein Society 2020; 29: 258–267

Boyle EA, O'Roak BJ, Martin BK, Kumar A, Shendure J. MIPgen: optimized modeling and design of molecular inversion probes for targeted resequencing. Bioinformatics (Oxford, England) 2014; 30: 2670–2672

Chen Z, Lei Y, Cao X, Zheng Y, Wang F, Bao Y, Peng R, Finnell RH, Zhang T, Wang H. Genetic analysis of Wnt/PCP genes in neural tube defects. BMC medical genomics 2018; 11: 38

Colin E, Huynh Cong E, Mollet G, Guichet A, Gribouval O, Arrondel C, Boyer O, Daniel L, Gubler M-C, Ekinci Z, Tsimaratos M, Chabrol B, Boddaert N, Verloes A, Chevrollier A, Gueguen N, Desquiret-Dumas V, Ferré M, Procaccio V, Richard L, Funalot B, Moncla A, Bonneau D, Antignac C. Loss-of-function mutations in WDR73 are responsible for

microcephaly and steroid-resistant nephrotic syndrome: Galloway-Mowat syndrome. American journal of human genetics 2014; 95: 637–648

Connaughton DM, Dai R, Owen DJ, Marquez J, Mann N, Graham-Paquin AL, Nakayama M, Coyaud E, Laurent EMN, St-Germain JR, Blok LS, Vino A, Klämbt V, Deutsch K, Wu C-HW, Kolvenbach CM, Kause F, Ottlewski I, Schneider R, Kitzler TM, Majmundar AJ, Buerger F, Onuchic-Whitford AC, Youying M, Kolb A, Salmanullah D, Chen E, van der Ven AT, Rao J, Ityel H, Seltzsam S, Rieke JM, Chen J, Vivante A, Hwang D-Y, Kohl S, Dworschak GC, Hermle T, Alders M, Bartolomaeus T, Bauer SB, Baum MA, Brilstra EH, Challman TD, Zyskind J, Costin CE, Dipple KM, Duijkers FA, Ferguson M, Fitzpatrick DR, Fick R, Glass IA, Hulick PJ, Kline AD, Krey I, Kumar S, Lu W, Marco EJ, Wentzensen IM, Mefford HC, Platzer K, Povolotskaya IS, Savatt JM, Shcherbakova NV, Senguttuvan P, Squire AE, Stein DR, Thiffault I, Voinova VY, Somers MJG, Ferguson MA, Traum AZ, Daouk GH, Daga A, Rodig NM, Terhal PA, van Binsbergen E, Eid LA, Tasic V, Rasouly HM, Lim TY, Ahram DF, Gharavi AG, Reutter HM, Rehm HL, MacArthur DG, Lek M, Laricchia KM, Lifton RP, Xu H, Mane SM, Sanna-Cherchi S, Sharrocks AD, Raught B, Fisher SE, Bouchard M, Khokha MK, Shril S, Hildebrandt F. Mutations of the Transcriptional Corepressor ZMYM2 Cause Syndromic Urinary Tract Malformations. American journal of human genetics 2020; 107: 727–742

Cooper DN, Krawczak M, Polychronakos C, Tyler-Smith C, Kehrer-Sawatzki H. Where genotype is not predictive of phenotype: towards an understanding of the molecular basis of reduced penetrance in human inherited disease. Human genetics 2013; 132: 1077–1130

Corsello G, Giuffrè M. Congenital malformations. The journal of maternal-fetal & neonatal medicine : the official journal of the European Association of Perinatal Medicine, the Federation of Asia and Oceania Perinatal Societies, the International Society of Perinatal Obstetricians 2012; 25 Suppl 1: 25–29

Cunningham F, Allen JE, Allen J, Alvarez-Jarreta J, Amode MR, Armean IM, Austine-Orimoloye O, Azov AG, Barnes I, Bennett R, Berry A, Bhai J, Bignell A, Billis K, Boddu

S, Brooks L, Charkhchi M, Cummins C, Da Rin Fioretto L, Davidson C, Dodiya K, Donaldson S, El Houdaigui B, El Naboulsi T, Fatima R, Giron CG, Genez T, Martinez JG, Guijarro-Clarke C, Gymer A, Hardy M, Hollis Z, Hourlier T, Hunt T, Juettemann T, Kaikala V, Kay M, Lavidas I, Le T, Lemos D, Marugán JC, Mohanan S, Mushtaq A, Naven M, Ogeh DN, Parker A, Parton A, Perry M, Piližota I, Prosovetskaia I, Sakthivel MP, Salam AIA, Schmitt BM, Schuilenburg H, Sheppard D, Pérez-Silva JG, Stark W, Steed E, Sutinen K, Sukumaran R, Sumathipala D, Suner M-M, Szpak M, Thormann A, Tricomi FF, Urbina-Gómez D, Veidenberg A, Walsh TA, Walts B, Willhoft N, Winterbottom A, Wass E, Chakiachvili M, Flint B, Frankish A, Giorgetti S, Haggerty L, Hunt SE, IIsley GR, Loveland JE, Martin FJ, Moore B, Mudge JM, Muffato M, Perry E, Ruffier M, Tate J, Thybert D, Trevanion SJ, Dyer S, Harrison PW, Howe KL, Yates AD, Zerbino DR, Flicek P. Ensembl 2022. Nucleic acids research 2022; 50: D988-D995

Drabkin HJ, RajBhandary UL. Initiation of protein synthesis in mammalian cells with codons other than AUG and amino acids other than methionine. Molecular and cellular biology 1998; 18: 5140–5147

Essner J, 2016: Zebrafish embryo microinjection Ribonucleoprotein delivery using the Alt-RTM CRISPR-Cas9 System. User Methods, IDT Inc. Coralville, IA, Integrated DNA Technologies. https://idtdevblob.blob.core.windows.net/sitefinity/docs/default-source/user-submitted-method/crispr-cas9-rnp-delivery-zebrafish-embryos-j-essnerc46b5a1532796e2eaa53ff00001c1b3c.pdf?sfvrsn=52123407_10 (Zugriffsdatum: 01.03.2024)

Goldenberg O, Erez E, Nimrod G, Ben-Tal N. The ConSurf-DB: pre-calculated evolutionary conservation profiles of protein structures. Nucleic acids research 2009; 37: D323-7

Greene NDE, Copp AJ. Neural tube defects. Annual review of neuroscience 2014; 37: 221–242

Grzegorski SJ, Chiari EF, Robbins A, Kish PE, Kahana A. Natural variability of Kozak sequences correlates with function in a zebrafish model. PloS one 2014; 9: e108475

Hsu P, Ma A, Wilson M, Williams G, Curotta J, Munns CF, Mehr S. CHARGE syndrome: a review. Journal of paediatrics and child health 2014; 50: 504–511

Jobst-Schwan T, Schmidt JM, Schneider R, Hoogstraten CA, Ullmann JFP, Schapiro D, Majmundar AJ, Kolb A, Eddy K, Shril S, Braun DA, Poduri A, Hildebrandt F. Acute multi-sgRNA knockdown of KEOPS complex genes reproduces the microcephaly phenotype of the stable knockout zebrafish model. PloS one 2018; 13: e0191503

Jumper J, Evans R, Pritzel A, Green T, Figurnov M, Ronneberger O, Tunyasuvunakool K, Bates R, Žídek A, Potapenko A, Bridgland A, Meyer C, Kohl SAA, Ballard AJ, Cowie A, Romera-Paredes B, Nikolov S, Jain R, Adler J, Back T, Petersen S, Reiman D, Clancy E, Zielinski M, Steinegger M, Pacholska M, Berghammer T, Bodenstein S, Silver D, Vinyals O, Senior AW, Kavukcuoglu K, Kohli P, Hassabis D. Highly accurate protein structure prediction with AlphaFold. Nature 2021; 596: 583–589

Kancherla V. Neural tube defects: a review of global prevalence, causes, and primary prevention. Child's nervous system : ChNS : official journal of the International Society for Pediatric Neurosurgery 2023; 39: 1703–1710

Köllges R, Stegmann J, Schneider S, Waffenschmidt L, Fazaal J, Breuer K, Hilger AC, Dworschak GC, Mingardo E, Rösch W, Hofmann A, Neissner C, Ebert A-K, Stein R, Younsi N, Hirsch-Koch K, Schmiedeke E, Zwink N, Jenetzky E, Thiele H, Ludwig KU, Reutter H. Exome Survey and Candidate Gene Re-Sequencing Identifies Novel Exstrophy Candidate Genes and Implicates LZTR1 in Disease Formation. Biomolecules 2023; 13

Li J, Lin S-M, Qiao J-D, Liu X-R, Wang J, Jiang M, Zhang J, Zhong M, Chen X-Q, Zhu J, He N, Su T, Shi Y-W, Yi Y-H, Liao W-P. CELSR3 variants are associated with febrile

seizures and epilepsy with antecedent febrile seizures. CNS neuroscience & therapeutics 2022; 28: 382–389

Lopes FM, Roberts NA, Zeef LA, Gardiner NJ, Woolf AS. Overactivity or blockade of transforming growth factor-β each generate a specific ureter malformation. The Journal of pathology 2019; 249: 472–484

Mingardo E, Beaman G, Grote P, Nordenskjöld A, Newman W, Woolf AS, Eckstein M, Hilger AC, Dworschak GC, Rösch W, Ebert A-K, Stein R, Brusco A, Di Grazia M, Tamer A, Torres FM, Hernandez JL, Erben P, Maj C, Olmos JM, Riancho JA, Valero C, Hostettler IC, Houlden H, Werring DJ, Schumacher J, Gehlen J, Giel A-S, Buerfent BC, Arkani S, Åkesson E, Rotstein E, Ludwig M, Holmdahl G, Giorgio E, Berettini A, Keene D, Cervellione RM, Younsi N, Ortlieb M, Oswald J, Haid B, Promm M, Neissner C, Hirsch K, Stehr M, Schäfer F-M, Schmiedeke E, Boemers TM, van Rooij IALM, Feitz WFJ, Marcelis CLM, Lacher M, Nelson J, Ure B, Fortmann C, Gale DP, Chan MMY, Ludwig KU, Nöthen MM, Heilmann S, Zwink N, Jenetzky E, Odermatt B, Knapp M, Reutter H. A genome-wide association study with tissue transcriptomics identifies genetic drivers for classic bladder exstrophy. Communications biology 2022; 5: 1203

Moreno-Mateos MA, Vejnar CE, Beaudoin J-D, Fernandez JP, Mis EK, Khokha MK, Giraldez AJ. CRISPRscan: designing highly efficient sgRNAs for CRISPR-Cas9 targeting in vivo. Nature methods 2015; 12: 982–988

Murugapoopathy V, Gupta IR. A Primer on Congenital Anomalies of the Kidneys and Urinary Tracts (CAKUT). Clinical journal of the American Society of Nephrology : CJASN 2020; 15: 723–731

Naylor RW, Qubisi SS, Davidson AJ. Zebrafish Pronephros Development. Results and problems in cell differentiation 2017; 60: 27–53

Rentzsch P, Witten D, Cooper GM, Shendure J, Kircher M. CADD: predicting the deleteriousness of variants throughout the human genome. Nucleic acids research 2019; 47: D886-D894

Reutter H, Keppler-Noreuil K, E Keegan C, Thiele H, Yamada G, Ludwig M. Genetics of Bladder-Exstrophy-Epispadias Complex (BEEC): Systematic Elucidation of Mendelian and Multifactorial Phenotypes. Current genomics 2016; 17: 4–13

Schmidt R, Strähle U, Scholpp S. Neurogenesis in zebrafish - from embryo to adult. Neural development 2013; 8: 3

Shima Y, Copeland NG, Gilbert DJ, Jenkins NA, Chisaka O, Takeichi M, Uemura T. Differential expression of the seven-pass transmembrane cadherin genes Celsr1-3 and distribution of the Celsr2 protein during mouse development. Developmental dynamics : an official publication of the American Association of Anatomists 2002; 223: 321–332

Sim N-L, Kumar P, Hu J, Henikoff S, Schneider G, Ng PC. SIFT web server: predicting effects of amino acid substitutions on proteins. Nucleic acids research 2012; 40: W452-7

Sobreira N, Schiettecatte F, Valle D, Hamosh A. GeneMatcher: a matching tool for connecting investigators with an interest in the same gene. Human mutation 2015; 36: 928–930

Stegmann JD, Kalanithy JC, Dworschak GC, Ishorst N, Mingardo E, Lopes FM, Ho YM, Grote P, Lindenberg TT, Yilmaz Ö, Channab K, Seltzsam S, Shril S, Hildebrandt F, Boschann F, Heinen A, Jolly A, Myers K, McBride K, Bekheirnia MR, Bekheirnia N, Scala M, Morleo M, Nigro V, Torella A, Pinelli M, Capra V, Accogli A, Maitz S, Spano A, Olson RJ, Klee EW, Lanpher BC, Jang SS, Chae J-H, Steinbauer P, Rieder D, Janecke AR, Vodopiutz J, Vogel I, Blechingberg J, Cohen JL, Riley K, Klee V, Walsh LE, Begemann M, Elbracht M, Eggermann T, Stoppe A, Stuurman K, van Slegtenhorst M, Barakat TS, Mulhern MS, Sands TT, Cytrynbaum C, Weksberg R, Isidori F, Pippucci T, Severi G, Montanari F, Kruer MC, Bakhtiari S, Darvish H, Reutter H, Hagelueken G,

Geyer M, Woolf AS, Posey JE, Lupski JR, Odermatt B, Hilger AC. Bi-allelic variants in CELSR3 are implicated in central nervous system and urinary tract anomalies. NPJ genomic medicine 2024; 9: 18

van der Ven AT, Connaughton DM, Ityel H, Mann N, Nakayama M, Chen J, Vivante A, Hwang D-Y, Schulz J, Braun DA, Schmidt JM, Schapiro D, Schneider R, Warejko JK, Daga A, Majmundar AJ, Tan W, Jobst-Schwan T, Hermle T, Widmeier E, Ashraf S, Amar A, Hoogstraaten CA, Hugo H, Kitzler TM, Kause F, Kolvenbach CM, Dai R, Spaneas L, Amann K, Stein DR, Baum MA, Somers MJG, Rodig NM, Ferguson MA, Traum AZ, Daouk GH, Bogdanović R, Stajić N, Soliman NA, Kari JA, El Desoky S, Fathy HM, Milosevic D, Al-Saffar M, Awad HS, Eid LA, Selvin A, Senguttuvan P, Sanna-Cherchi S, Rehm HL, MacArthur DG, Lek M, Laricchia KM, Wilson MW, Mane SM, Lifton RP, Lee RS, Bauer SB, Lu W, Reutter HM, Tasic V, Shril S, Hildebrandt F. Whole-Exome Sequencing Identifies Causative Mutations in Families with Congenital Anomalies of the Kidney and Urinary Tract. Journal of the American Society of Nephrology : JASN 2018; 29: 2348–2361

Vivante A, Kohl S, Hwang D-Y, Dworschak GC, Hildebrandt F. Single-gene causes of congenital anomalies of the kidney and urinary tract (CAKUT) in humans. Pediatric nephrology (Berlin, Germany) 2014; 29: 695–704

Wang S, Mandell JD, Kumar Y, Sun N, Morris MT, Arbelaez J, Nasello C, Dong S, Duhn C, Zhao X, Yang Z, Padmanabhuni SS, Yu D, King RA, Dietrich A, Khalifa N, Dahl N, Huang AY, Neale BM, Coppola G, Mathews CA, Scharf JM, Fernandez TV, Buxbaum JD, Rubeis S de, Grice DE, Xing J, Heiman GA, Tischfield JA, Paschou P, Willsey AJ, State MW. De Novo Sequence and Copy Number Variants Are Strongly Associated with Tourette Disorder and Implicate Cell Polarity in Pathogenesis. Cell reports 2018; 24: 3441-3454.e12

Wang X-J, Zhang D-L, Xu Z-G, Ma M-L, Wang W-B, Li L-L, Han X-L, Huo Y, Yu X, Sun J-P. Understanding cadherin EGF LAG seven-pass G-type receptors. Journal of neurochemistry 2014; 131: 699–711

Wiel L, Baakman C, Gilissen D, Veltman JA, Vriend G, Gilissen C. MetaDome: Pathogenicity analysis of genetic variants through aggregation of homologous human protein domains. Human mutation 2019; 40: 1030–1038

Zhou L, Bar I, Achouri Y, Campbell K, Backer O de, Hebert JM, Jones K, Kessaris N, Rouvroit CL de, O'Leary D, Richardson WD, Goffinet AM, Tissir F. Early forebrain wiring: genetic dissection using conditional Celsr3 mutant mice. Science (New York, N.Y.) 2008; 320: 946–949

2. Veröffentlichung

Reproduced with permission from Springer Nature.

Reference to original publication:

Stegmann, J.D., Kalanithy, J.C., Dworschak, G.C. et al. Bi-allelic variants in *CELSR3* are implicated in central nervous system and urinary tract anomalies. npj Genom. Med. 9, 18 (2024). https://doi.org/10.1038/s41525-024-00398-9

Published in partnership with CEGMR, King Abdulaziz University

https://doi.org/10.1038/s41525-024-00398-9

Bi-allelic variants in *CELSR3* are implicated in central nervous system and urinary tract anomalies

Check for updates

Jil D. Stegmann[1,2,63] ✉, Jeshurun C. Kalanithy[1,3,63], Gabriel C. Dworschak[1,3,4], Nina Ishorst[1,3], Enrico Mingardo[2], Filipa M. Lopes[5], Yee Mang Ho[5], Phillip Grote[6], Tobias T. Lindenberg[3], Öznur Yilmaz[3], Khadija Channab[2], Steve Seltzsam[7], Shirlee Shril[7], Friedhelm Hildebrandt[7], Felix Boschann[8], André Heinen[9], Angad Jolly[10,11], Katherine Myers[12], Kim McBride[12], Mir Reza Bekheirnia[10,13], Nasim Bekheirnia[13,14], Marcello Scala[15,16], Manuela Morleo[17,18], Vincenzo Nigro[17,18], Annalaura Torella[17,18], TUDP consortium*, Michele Pinelli[18,19], Valeria Capra[20], Andrea Accogli[21,22], Silvia Maitz[23], Alice Spano[24], Rory J. Olson[25], Eric W. Klee[25,26,27], Brendan C. Lanpher[25,26], Se Song Jang[28], Jong-Hee Chae[28,29], Philipp Steinbauer[30], Dietmar Rieder[31], Andreas R. Janecke[32,33], Julia Vodopiutz[34], Ida Vogel[35,36], Jenny Blechingberg[36], Jennifer L. Cohen[37], Kacie Riley[38], Victoria Klee[39], Laurence E. Walsh[39], Matthias Begemann[40], Miriam Elbracht[40], Thomas Eggermann[40], Arzu Stoppe[41], Kyra Stuurman[42], Marjon van Slegtenhorst[42], Tahsin Stefan Barakat[42], Maureen S. Mulhern[43,44], Tristan T. Sands[45,46,47], Cheryl Cytrynbaum[48,49], Rosanna Weksberg[49,50], Federica Isidori[51], Tommaso Pippucci[51], Giulia Severi[51], Francesca Montanari[51], Michael C. Kruer[52,53], Somayeh Bakhtiari[52,53], Hossein Darvish[54], Heiko Reutter[1,55,56], Gregor Hagelueken[57], Matthias Geyer[57], Adrian S. Woolf[5,58], Jennifer E. Posey[10], James R. Lupski[10,14,59,60], Benjamin Odermatt[2,3,64] & Alina C. Hilger[61,62,64] ✉

CELSR3 codes for a planar cell polarity protein. We describe twelve affected individuals from eleven independent families with bi-allelic variants in *CELSR3*. Affected individuals presented with an overlapping phenotypic spectrum comprising central nervous system (CNS) anomalies (7/12), combined CNS anomalies and congenital anomalies of the kidneys and urinary tract (CAKUT) (3/12) and CAKUT only (2/12). Computational simulation of the 3D protein structure suggests the position of the identified variants to be implicated in penetrance and phenotype expression. CELSR3 immunolocalization in human embryonic urinary tract and transient suppression and rescue experiments of Celsr3 in fluorescent zebrafish reporter lines further support an embryonic role of *CELSR3* in CNS and urinary tract formation.

Co-occurrence of congenital anatomical and functional anomalies of the central nervous system (CNS) and congenital anomalies of the kidneys and urinary tract (CAKUT) have been previously reported, e.g. Galloway-Mowat syndrome [MIM 251300][1]; CAKUTHED [MIM 617641][2]; or NECRC [MIM 619522][3]. The cadherin EGF LAG seven-pass G-type receptors (CELSRs) are as a subgroup of adhesion G protein-coupled receptors (aGPCRs) involved in many biological processes such as regulation of planar cell polarity (PCP) during embryonic development, neuronal and endocrine cell differentiation, vessel formation and axon guidance[4,5]. In the context of kidney development and pathophysiology, aGPCRs and in particular Celsr1 are known to play an important role in ureteric bud branching[6]. All CELSR family members CELSR1-3 have large ecto-domains for homophilic interactions followed by seven transmembrane segments and a cytoplasmic domain[4]. Expression studies of all three CELSR paralogs in xenopus and mice show distinct co-expression in the embryonic CNS and the pronephric system, a vertebrate kidney precursor[6–8]. *Celsr3* mutant mice show severe thalamocortical disconnection, decreased rubrospinal axons, corticospinal axons, spinal motoneurons and neuromuscular junctions, due

A full list of affiliations appears at the end of the paper. *A list of authors and their affiliations appears at the end of the paper. ✉e-mail: jil.stegmann@uni-bonn.de; alina.hilger@uk-erlangen.de

to failure in axon guidance or outgrowth[9–11]. Rare monoallelic variants in human *CELSR3* have been associated with neural tube defects (NTDs)[4,12], febrile seizures[13] and Tourette disorder[14].

Previously, we detected compound heterozygous variant alleles in *CELSR3* in an affected female with CAKUT and tethered cord syndrome[15]. Here, we report a total of twelve individuals with rare or novel bi-allelic variants in *CELSR3*. The affected individuals share an overlapping phenotypic spectrum comprising CNS anomalies, co-occurring CNS anomalies combined with CAKUT and CAKUT only. Computational simulation of the 3D protein structure suggests the position of the identified variants to be implicated in phenotype expression. Immuno-detection of CELSR3 in human embryonic urinary tract and transient suppression and rescue experiments of Celsr3 in fluorescent zebrafish reporter lines suggest an embryonic involvement in CNS and urinary tract formation.

Results

Individuals with bi-allelic variants in *CELSR3* present within a phenotypic spectrum

Six of the twelve described individuals presented with homozygous missense and five with compound heterozygous missense *CELSR3* variant alleles (Table 1). Individual 5: II-2 carried a heterozygous missense variant and an in-frame-deletion in trans. Seven of twelve individuals presented with a predominant CNS phenotype (1: II-1, 2: II-1, 2: II-2, 3: II-1, 4: II-3, 5: II-2, 6: II-1), three presented with a combined CNS and CAKUT phenotype (7: II-1, 8: II-1, 9: II-1) and two presented with CAKUT only (10: II-1, 11: II-1) (Table 1, Fig. 1).

Individuals with predominant CNS or combined CNS and CAKUT phenotypes presented with intellectual disability and/or developmental delay (ID / DD), hypotonia, seizures, brain malformations, NTDs, macro- or microcephaly (occipitofrontal circumference ±2 SD). The CAKUT spectrum in individuals with combined CNS and CAKUT or CAKUT only comprised duplicated collecting system, ectopic kidney, multi-cystic dysplastic kidney, vesico-ureteric reflux, hydronephrosis, obstructive uropathies or irregular bladder wall. Detailed phenotype information can be found in Table 1 and Supplement B.

In silico analysis predicts intolerance of *CELSR3* variants

In individuals with a predominant CNS phenotype, eight out of ten variants were characterized as presumably damaging by at least two in silico prediction tools. One of these ten variants was predicted to be presumably damaging by all three prediction tools. All these variants affect residues highly conserved among species (Fig. 1a) and are annotated with a CADD score above 22, except for c.8480C>A (CADD score 17.8) (Table 1).

In individuals with CNS and CAKUT, and CAKUT only phenotype, five out of six identified variants were characterized as presumably damaging by at least two in silico prediction tools, four of these six variants were predicted to be presumably damaging by all three prediction tools. All these variants are annotated with a CADD score above 22 (Table 1) and affect highly conserved residues, except for c.3142C>T (Fig. 1b).

Structural modeling reveals phenotype associated distribution of CELSR3 protein variants

We used PhosphositePlus[16] and AlphaFold[17] to create a model of the 3312 amino acid (aa) human CELSR3 protein using a ´divide-and-conquer´ strategy. The N-terminus of the protein comprises 307 aa (1–307) and the C-terminus contains 522 aa (2790–3312) for which no structural modeling was possible as no suitable homology template exists. CELSR3 contains seven membrane spanning helices (aa 2541–2774), which are part of the modeled section of this protein. The location of variants was mapped onto the model (Fig. 2). According to this modeling most modeled variants are predicted to potentially destabilize the respective region or affect the possible interaction surface due to changes in polarity or structure (Supplementary Table 1).

Only three of the ten variants found in individuals with a predominant CNS phenotype localize N-terminal in distance to the membrane associated domains. Whereas seven out of ten possibly CNS associated variants cluster within the perimembraneous domains and in the intracellular C-terminal domain (Fig. 2). Remarkably, the p.Ile2409del variant introduces a register shift into the side chain up-down sequence of a beta strand, potentially leading to a larger structural disturbance in this area. The p.Gly2667Ser variant is in an extracellular loop of the transmembrane domain and the variation to a polar serine can change the interaction surface of this region.

In comparison, all variants identified in individuals with CAKUT reside within extracellular N-terminal domains, including individuals 10: II-1 and 11: II-1 with variants in similar positions in one of the Cadherin domains (p.Arg1048Trp and p.Glu1034Gln) and similar CAKUT only phenotype (Table 1; Fig. 2). Two of these six possibly CAKUT associated variants cluster close to the GAIN-GPS motif: p.Val2320Ala, p.Glu2501Lys. The variant p.Val2320Ala might induce conformational changes of that loop in the GAIN domain and p.Glu2501Lys could significantly affect interactions by changes in polarity. Due to the absence of available research data, it was not possible to structurally model the cytoplasmic domains of CELSR3 (>500 aa). Interestingly, three of the in total 16 variants in twelve individuals identified in this study are located in this comparably small cytoplasmic area of the protein, suggesting this unresearched region to be important for protein function as well (Fig. 2).

Detection of CELSR3 in the human embryonic metanephric kidney and urinary tract

CELSR3 was immuno-detected in different structures of the human embryonic metanephros, the precursor of the human kidney (Fig. 3, Supplementary Fig. 2). Similar patterns of CELSR3 were noted in metanephric kidneys at ten and twelve weeks of gestation. CELSR3 was detected in medullary collecting ducts and in ureteric bud branch stalks in the cortex of the developing organ. The protein was further detected in the Bowman capsule of immature glomeruli and there was weak immunostaining in proximal tubules. At the same stage, uncondensed metanephric mesenchyme in the outer cortex immuno-stained for CELSR3 as well (Fig. 3). In sections of a seven-week human embryo, CELSR3 was immuno-detected in epithelia of both the urogenital sinus tube, the precursor of the bladder urothelium, and also epithelia of the hindgut (Supplementary Fig. 2). The seven-week metanephric kidney contains a central ureteric stalk, with its branch tips capped by condensing metanephric mesenchyme, containing the nephron precursor cells. Neither of these showed a significant signal for CELSR3. But uncondensed metanephric mesenchyme in the seven-week metanephros stained for CELSR3. In addition, large (proximal) tubules in the adjacent mesonephros immuno-stained for CELSR3 as well (Supplementary Fig. 2).

Transient suppression of CELSR3 ortholog Celsr3 in zebrafish leads to anomalies in the developing CNS and urinary system

The similarity between the human CELSR3 protein and the zebrafish (zf) ortholog Celsr3 regarding all four described zf transcripts (*celsr3-201*, *celsr3-202*, *celsr3-203* and *celsr3-204*) is ~78% (2316/2959 aa) (SerialCloner 2.6.1 software). PCR amplification of the 5' end of *celsr3* from zf cDNA revealed a larger transcribed region of at least an additional 2,138 base pairs (bp) compared to that previously described *celsr3-204*. Morpholino® knockdown (MO-KD) with the translational-blocking MO (TB-MO) targeted to the start codon 195 bp upstream of zf mRNA-transcript *celsr3-204* (TB-MO-204) as well as the splice-blocking MO (SB-MO-e6i6) both showed a matching phenotype during the first five days post fertilization (dpf) (Fig. 4, Supplementary Fig. 3). We defined the phenotype as a warped tail partly in combination with a disruption of neuronal or musculoskeletal tissue at the caudal end from two dpf onwards. This phenotype was significantly more frequent in SB-MO-e6i6-treated zf larvae (zfl) (42%) and TB-MO-204-treated zfl (83%) compared to Control-MO-treated zfl (2%, two-way ANOVA, p as indicated) (Fig. 4a, b, Supplementary Fig. 3). The co-injection of TB-MO-204 with human wild-type (wt) *CELSR3* polyA mRNA reduced this phenotype to 23% of zfl. Hence in most TB-MO-204-treated zfl the phenotype could be rescued with human wt mRNA of *CELSR3*.

Table 1 | Clinical and molecular data of individuals with bi-allelic variants in *CELSR3*

	Individual	ZYG	Variant	MAF	CADD; P; S; M	ID / DD	Tonus	Seizures	Brain, NTD	OFC	CAKUT	Other
CNS	**1: II-1**	CH	c.1574G>A, p.(Arg525His)	2.31e-5	27.5; 3; D; T	DD	np	np	np	-2.21 z	np	Atopic dermatitis, frequent febrile infections
			c.9299G>C, p.(Gly3100Ala)	NR	24.8; 2; D; HT							
	2: II-1	CH	c.7423C>T, p.(Arg2475Trp)	6.57e-5	28.1; 3; D; N	ID, DD	Central hypotonia	BNS seizures, DEE	np	np	np	Neonatal hypoglycaemia, TTTS (acceptor), FTT, facial dysmorphism
			c.8758C>T, p.(Arg2920Trp)	1.97e-5	25.7; 1; D; HT							
	2: II-2	CH	c.7423C>T, p.(Arg2475Trp)	6.57e-5	28.1; 3; D; N	ID, DD	Central hypotonia	BNS seizures, DEE	Delayed opercularisation	np	np	Neonatal hypoglycaemia, TTTS (donor), FTT, facial dysmorphism
			c.8758C>T, p.(Arg2920Trp)	1.97e-5	25.7; 1; D; HT							
	3: II-1	Hom	c.6304G>A, p.(Ala2102Thr)	NR	24.1; 1; D; SI	Global DD	Hypotonia	LGS	Prominence of subarachnoid spaces	np	X	Strabismus, sleep disturbance
	4: II-3	CH	c.5059C>T, p.(His1687Tyr)	1.97e-5	23.6; 1; D; SI	ID	Hypotonia	Seizures	Pachygyria, double cortex	np	X	X
			c.7075C>T, p.(Pro2359Ser)	1.98e-5	23.3; 2; T; SI							
	5: II-2	CH	c.7224_7226del, (p.Ile2409del)	1.32e-5	25.3; NR; NR; I	PSM-R	np	np	X	np	X	Autoaggressivity, autism-spectrum-disorder, stereotypies, pectus excavatum, facial dysmorphism
			c.8480C>A, (p.Thr2827Asn)	NR	17.8; 3; D; T							
	6: II-1	Hom	c.7999G>A, p.(Gly2667Ser)	NR	26.5; 3; D; I	ID, DD	np	np	Hairy naevus lumbal	np	np	Obesity, facial dysmorphism, stereotypies, sleep disturbance
CNS +CAKUT	**7: II-1**	Hom	c.6959T>C, p.(Val2320Ala)	NR	27.2; 3; D; SI	np	np	np	Polymicrogyria, subependymal heterotopia	np	MCDK, contralateral compensatory hypertrophy	X
	8: II-1	Hom	c.4034C>T, p.(Pro1345Leu)	2.63e-5	22.8; 1; T; SI	DD	Hypotonia and joint laxity	Generalized seizures	Obstructive hydrocephalus, ACC, cerebral hypoplasia	+2.31 z	Unilateral ectopic kidney	Rib deformities, ASD, sensorineural hearing loss, growth retardation, facial dysmorphism
	9: II-1	CH	c.3712C>T, p.(Arg1238Cys)	6.57e-6	28.2; 3; D; I	ID, DD	Asymmetric motor exam	Complex febrile seizures	Chiari I, L, periventricular cysts, fatty filum / TCS	+1.55 z	Duplicated collecting system, irregular bladder wall	Anxiety, facial dysmorphism
			c.7501G>A, p.(Glu2501Lys)	3.94e-5	25; 3; D; I							
CAKUT	**10: II-1**	Hom	c.3142C>T, p.(Arg1048Trp)	3.29e-5	23; 3; D; SI	np	np	np	X	np	Bilateral VUR, duplicated collecting system	X
	11: II-1	Hom	c.3100G>C, p.(Glu1034Gln)	7.23e-5	23.3; 2; T; I	np	np	np	X	np	Bilateral UPJO, hydronephrosis, reduced kidney function, diffuse bladder wall thickening	X

Overview of clinical and molecular data of twelve individuals from eleven independent families with bi-allelic variants in *CELSR3*. Further details, as well as information on three families which are not included in the main text, can be found in Supplement A and B. *CNS* central nervous system, *CAKUT* congenital anomalies of the kidneys and urinary tract, *ZYG* zygosity, *CH* compound heterozygous, *Hom* homozygous, *MAF* minor allele frequency in gnomAD v3.1, *NR* not reported, *P* PolyPhen-2 (*1* benign, *2* possibly damaging, *3* probably damaging), *S* SIFT (*T* tolerated, *D* deleterious), *M* MetaDome (*HT* highly tolerant, *T* tolerant, *N* neutral, *SI* slightly intolerant, *I* intolerant), *ID* intellectual disability, *DD* developmental delay, *PSM-R* psychomotor regression, *BNS* Blitz-Nick-Salaam, *DEE* developmental and epileptic encephalopathy, *LGS* Lennox-Gastaut syndrome, *NTD* neural tube defect, *ACC* agenesis of corpus callosum, *L* leukoencephalopathy, *TCS* tethered cord syndrome, *OFC* occipitofrontal circumference, *MCDK* multicystic dysplastic kidney, *VUR* vesicoureteral reflux, *UPJO* ureteropelvic junction obstruction, *TTTS* twin-to-twin transfusion syndrome, *FTT* failure to thrive, *ASD* atrial septal defect, *np* phenotype not present, *X* not investigated.

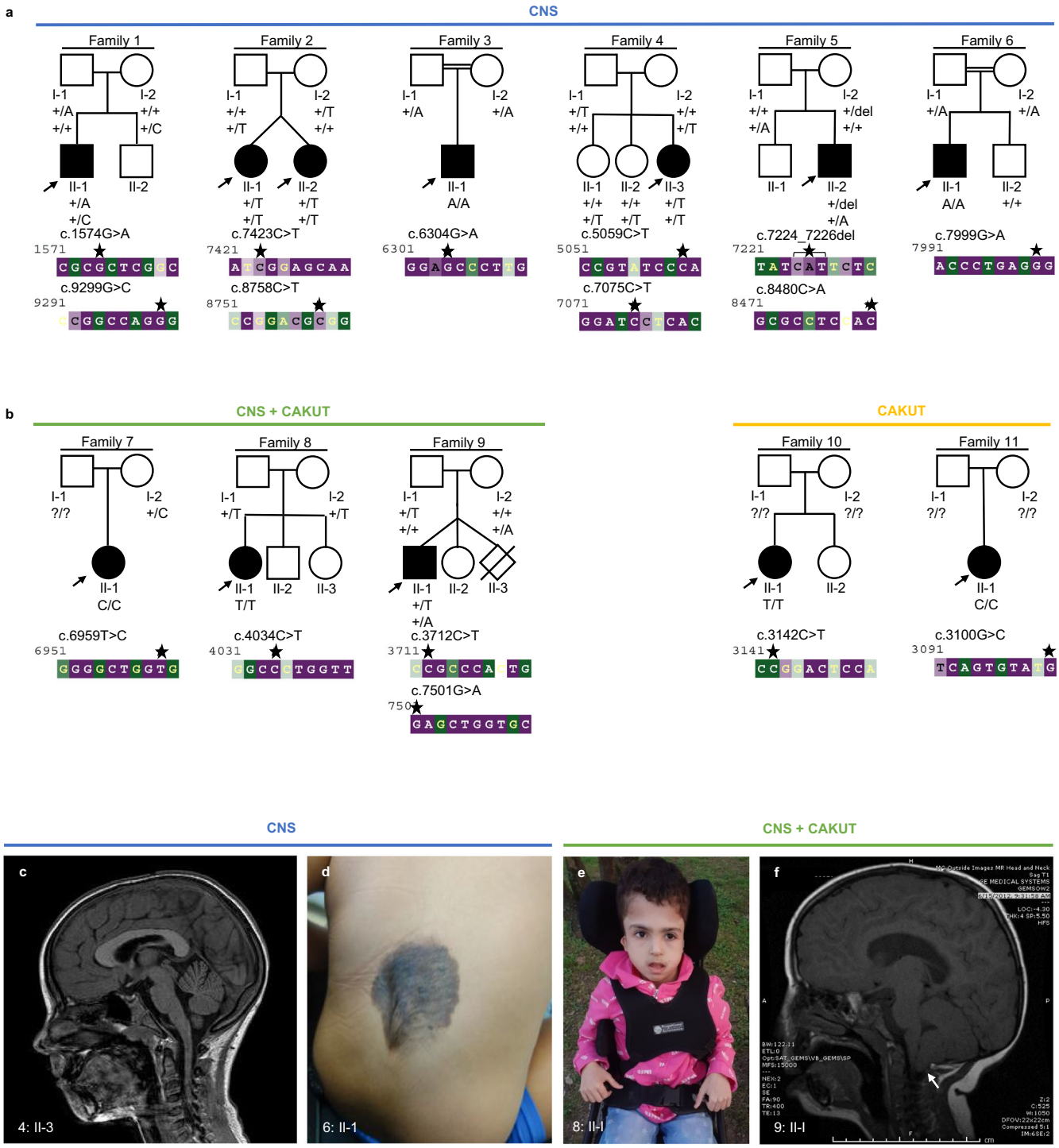

Fig. 1 | Families with bi-allelic variants in *CELSR3* and clinical images. **a** Pedigrees of six families (1–6) with a predominant central nervous system (CNS) phenotype. **b** Pedigrees of three families (7–9) with combined CNS phenotype and congenital anomalies of the kidneys and urinary tract (CAKUT), and two families (10, 11) with CAKUT only. The evolutionary conservation of the affected sequence (bp) was estimated with the ConSurf server from variable (green) to conserved (purple). Asterisks: Position of the respective variants. The arrows indicate probands. Filled shapes should reflect affected status. **c** Brain magnetic resonance image (MRI) of 4: II-3 showing pachygyria. **d** Photograph of 6: II-1 showing a congenital hairy melanocytic nevus with a diameter of 0.1 to 0.15 meter at the level of the lower lumbal spine. Radiologic imaging of the spine was not performed here. **e** Photograph of 8: II-1 showing macrocephaly, high and prominent forehead and very small and low-set ears. **f** MRI of 9: II-1. Arrow: Chiari malformation type 1 (cerebellar tonsillar herniation).

Furthermore, we could show that there is no significant difference between rescued and Control-MO-treated zfl.

In a parallel approach, we injected a CRISPR-Cas9 mix into zf embryos with six sgRNAs targeting *celsr3*. A comparable phenotype to Celsr3 MO-KD zfl could be replicated in these *celsr3* F0 CRISPR knockout (KO) zfl, as well as a significant increase of affected zfl (63%) compared to scrambled controls (2%) (Fig. 4a, b). Of note, no significant differences in survival rates among MO-KD, rescue and control groups were observed within the first five dpf. However, *celsr3* F0 CRISPR KO zfl presented with a lower survival rate compared to scrambled controls (Fig. 4d). Using transgenic *Tg(-*

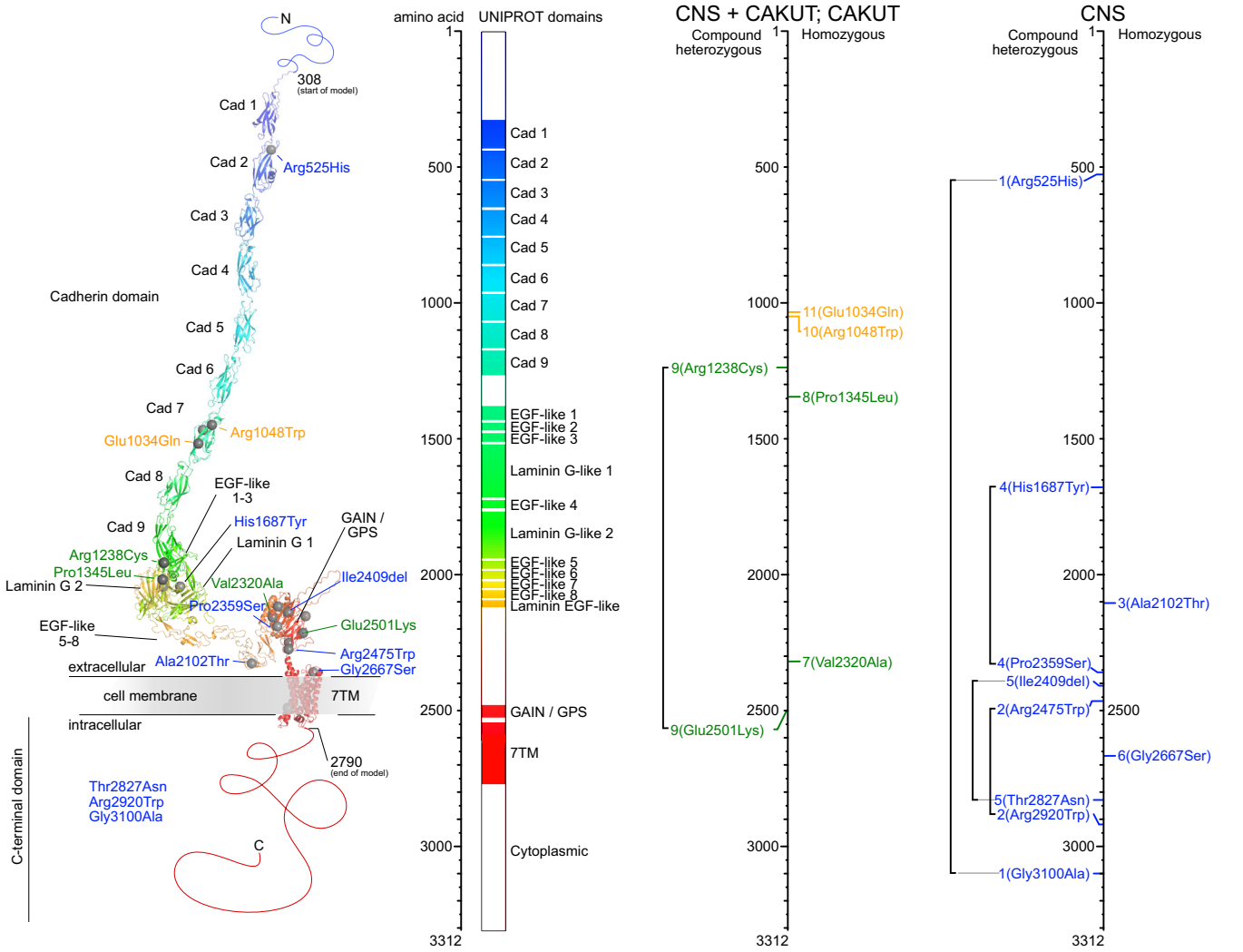

Fig. 2 | Structural modeling of CELSR3 and mapping of the variants. Structural modeling of CELSR3 and the respective variants according to the amino acid (aa) position. Left panel: 3D protein domain view and variant annotation using AlphaFold and PyMOL. Middle panel: Linearized aa view of the protein domains. Right panels: Variant location according to the respective phenotype categories: Central nervous system (CNS) anomalies in blue, combined CNS and congenital anomalies of the kidneys and urinary tract (CAKUT) in green, CAKUT only in yellow. Cad Cadherin, EGF Epidermal growth factor, GAIN G-protein-coupled receptor (GPCR) autoproteolysis-inducing domain, GPS GPCR proteolysis site, 7TM Seven-transmembrane.

3.1ngn1:GFP) zfl at three dpf we visualized the disrupted arrangement of proliferating neuronal progenitor cells and decreased axonal outgrowth in Celsr3 KD or KO zfl (Fig. 4c). We further evaluated the structural development of the pronephros in transgenic *Tg(wt1b:EGFP)* zfl at three dpf (Fig. 4e, Supplementary Fig. 3). Here, TB-MO-treated zfl showed a significant dilatation of the glomerulus and a reduced size of the neck segments, compared to controls. This effect was almost completely rescued after co-injection of TB-MO-204 together with human wt *CELSR3* polyA mRNA (Fig. 4f).

Discussion

In this study, we report twelve individuals from eleven independent families with rare or novel bi-allelic variants in *CELSR3* (Fig. 1, Table 1), most of them are missense variant alleles by conceptual translation.

Seven of ten variants of individuals with a predominant CNS phenotype reside in the intracellular or the peri-membranous protein region, including the GAIN and GPS domain (Fig. 2). The highly conserved GPCR-Autoproteolysis Inducing (GAIN) domain is structurally and functionally linked to the GPCR-Proteolysis Site (GPS) by mediating a chemical environment in the GPS necessary for autoproteolysis[18]. The intracellular C-terminal fragment (CTF) in GPCRs was found important for receptor density on the cell surface[19], PCP[20], and neural tube development[12,21,22]. Structural variation in the intracellular CTF of CELSR3 might impair receptor signaling predominantly leading to a CNS phenotype. Interestingly, all variants of individuals with a combined CNS and CAKUT or CAKUT only phenotype distribute within the extracellular domains. The extracellular cadherin repeats of CELSRs have adhesive properties and provide a likely structural mechanism for calcium-regulated interaction[4,5]. Our computed model of the human CELSR3 protein predicted potential structural and functional disturbances as a potential consequence of these respective extracellular or transmembrane variations (Fig. 2 and Supplementary Table 1). While these domains are structurally well characterized and allow quite precise calculation, intracellular variants are limited in structural interpretation due to sparse common information on the three-dimensional structure of the CTF. As indicated in the introduction, (rare) monoallelic variants in *CELSR3* have been described to be involved in neural tube defects (NTDs)[4,12], febrile seizures[13] and Tourette disorder[14]. However, the respective studies do not provide functional evidence to support this associations beyond doubt. Based on all available data, the protein was modeled and the effects of the identified variants were hypothetically

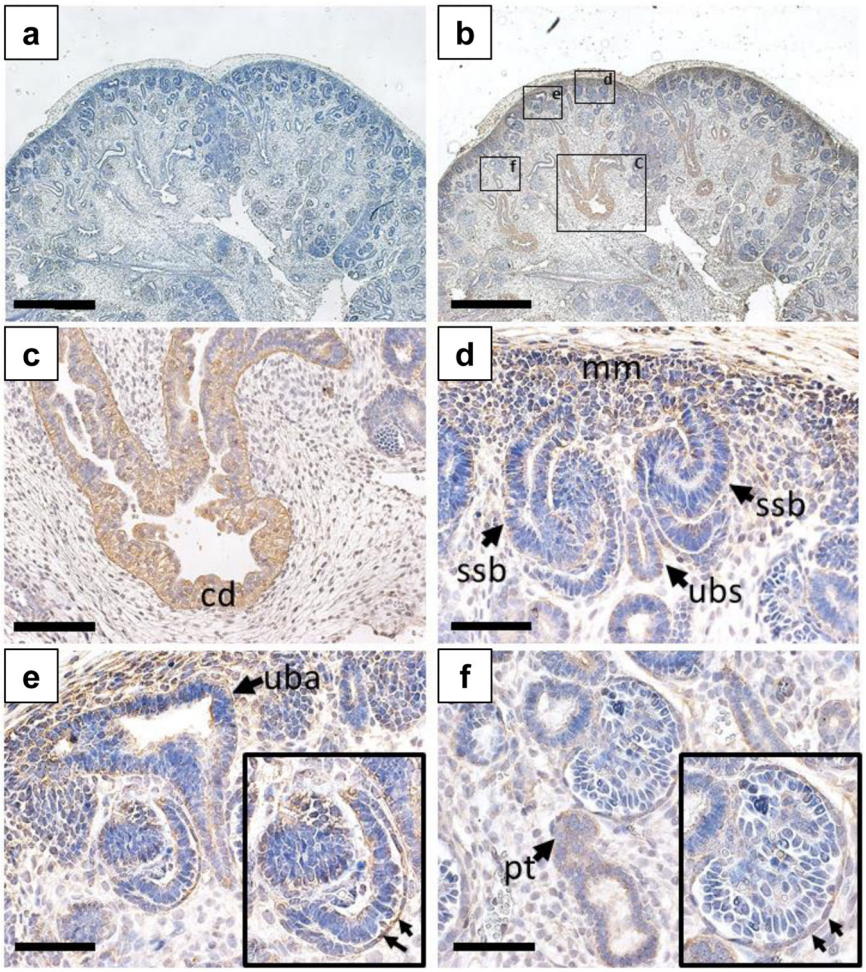

Fig. 3 | CELSR3 immunostaining in the human embryonic metanephric kidney at ten weeks gestation. All frames depict a ten-week gestation kidney with nuclei counterstained (blue) with hematoxylin. **a** Low power view of midsagittal section with primary antibody omitted. The nephrogenic cortex is uppermost and the medulla is in the low part of the image. Note the absence of brown color. **b** Adjacent section to that depicted in **a**. but immuno-stained for CELSR3. Note the positive signal *(brown)* in diverse structures. Boxed areas are detailed in **c**-**f**. **c** CELSR3 was detected in branching medullary collecting ducts *(cd)*. **d** The nephrogenic cortex contains immature structures. CELSR3 was detected in the ureteric bud branch stalk *(ubs)* which is flanked by nephron precursors called S-shape bodies *(ssb)*. The metanephric mesenchyme *(mm)* stained weakly for CELSR3. **e** Another view of the nephrogenic cortex showing the ureteric bud branch ampullary tip *(uba)*. These epithelia were weakly positive for CELSR3. Lower in the same image is an immature glomerulus with prominent CELSR3 immunostaining in the Bowman capsule, or parietal epithelia (arrows in the boxed enlargement). **f** The Bowman capsule of a more mature glomerulus has downregulated CELSR3 (arrows in boxed enlargement), and there is weak immunostaining in a nearby proximal tubule *(pt)*. Bars are 2 mm in frames **a** and **b**, and 200 µm in frames **c**–**f**.

outlined, implying certain limitations. Nevertheless, a limiting factor for the disease-gene relationship is that uncertainty remains about the specific function of the respective variants in the disease formation. Here identification of a larger cohort of affected biallelic variant carriers for further assessment is warranted. Furthermore, exploration of the respective variants in functional studies and cellular models are a direction for future research.

Previous studies indicated expression of Celsr3 protein in the CNS and disrupted axonal guidance in the forebrain of *Celsr3* conditional KO mice[8–10]. This led to a variety of developmental phenotypes of the CNS in these mice, which is in line with the phenotypic variability observed in our patients. While expression of Celsr3 in the developing CNS of mice was described previously[8–10], we extended the expression profile of *CELSR3/Celsr3* to the embryonic and fetal bladder precursor tissues using human and mouse transcriptome data (GEO accession ID: GSE190641; Supplementary Fig. 1)[23]. These findings suggest a conserved role of *CELSR3/Celsr3* not only during CNS but also during urinary tract development in vertebrates (Supplementary Fig. 1). Furthermore, we immuno-detected CELSR3 in different embryonic structures of the developing human metanephric kidney and the urogenital sinus epithelium of the nascent bladder (Fig. 3 and Supplementary Fig. 2). The postulate that CELSR3 has critical roles in the growth and differentiation of these diverse cell types is consistent with the range of malformations described here (i.e., dysplastic and fused collecting systems).

In order to investigate not only expression but also the role of CELSR3 in development, we chose the zfl as a model organism. The similarity of the human CELSR3 protein compared to the zf ortholog Celsr3 is notably high with 78% (2316/2959 aa). The PCP core component pathway is mediated in part by the Celsr1-3 subfamily, conserved through mice and zf[24]. Relative expression data in zfl from one hour post fertilization (hpf) to 21 dpf indicated the highest expression of *celsr3* at three dpf[24]. Therefore, we examined the function of Celsr3 during early development in a MO-KD and F0 CRISPR-Cas9 KO zf model. The zf transcript *celsr3-204* is described to begin protein synthesis with glutamate (GAA), even though protein synthesis is initiated commonly with AUG methionine codons[25]. The AUG translational start site of transcript *celsr3-204* that we detected 195 bp upstream of the previously described beginning of exon 1 shows a high similarity to the human 5‘ translational start site of *CELSR3* and a strong Kozak consensus (Kozak: ACCAUGGCG; *celsr3-204* minus 195 bp: AGCAUGGAG). Therefore, we designed a TB-MO targeting this probable AUG translational start site of transcript *celsr3-204* (TB-MO-204).

Transient suppression of *celsr3* transcripts in fluorescent zfl reporter lines demonstrates the function of Celsr3 during early embryonic CNS and urinary tract development (Fig. 4, Supplementary Fig. 3). Previously, the expression of *celsr3* has been described in primary neural clusters of the brain and the spinal cord in zfl starting at twelve hpf[26]. We characterized the effect of Celsr3 MO-KD and *celsr3* F0 CRISPR KO on neurogenesis using the fluorescent reporter line *Tg(-3.1ngn1:GFP)* (Fig. 4c). The structural irregularities at the caudal end and disrupted neuronal migration in zfl morphants possibly resemble the neuronal anomalies described in individuals 2: II-2, 4: II-3, 6: II-1, 7: II-1, 8: II-1 and 9: II-1 (Table 1). Since five of the here described individuals presented with CAKUT, we chose the transgenic *Tg(wt1b:EGFP)* zf line as a vertebrate model system to analyze the effect of Celsr3 MO-KD on the early urinary tract development[27]. These zfl showed structural anomalies of the developing pronephros in Celsr3 zf

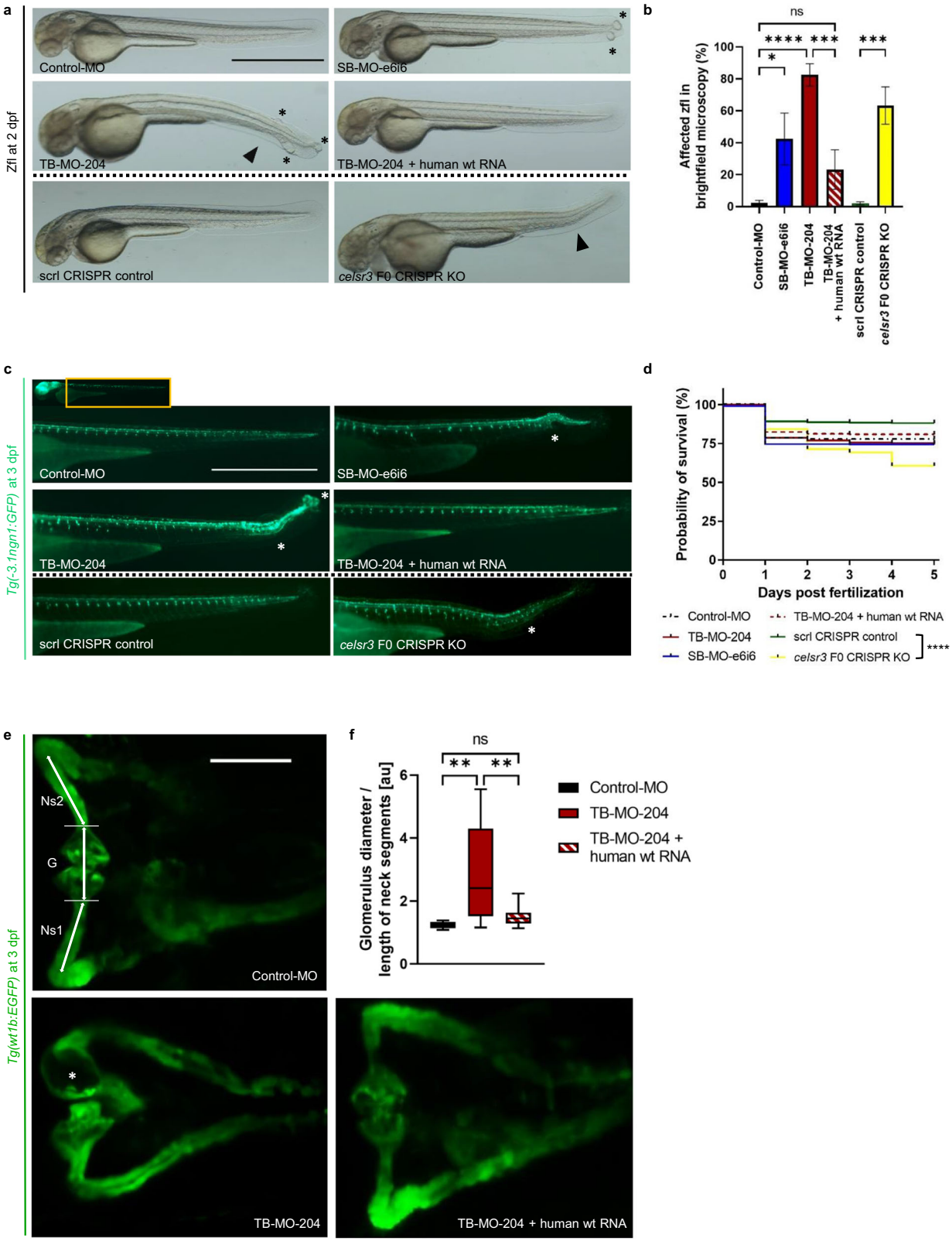

morphants at three dpf (Fig. 4e, f, Supplementary Fig. 3). We classified the disproportionally enlarged glomerulus as a marker for disturbed development of the pronephros and the urinary tract, comparable to the kidney anomalies including hydronephrosis, obstructive uropathies and other CAKUT phenotypes observed in this study (Table 1).

In conclusion, the presented human genomic and immunohistochemical results, computational simulation of protein structure, and functional studies in zfl, collectively support the hypothesis that bi-allelic variants in *CELSR3* are involved in a probable genetic disease mainly affecting the CNS and urinary tract.

Fig. 4 | Transient suppression of Celsr3 in zebrafish larvae. Phenotypic evaluation of the different zebrafish larvae (zfl) groups: Zfl injected with Control-Morpholino (Control-MO), zfl injected with MO blocking *celsr3* splice site exon 6 – intron 6 (SB-MO-e6i6), zfl injected with MO blocking transcript *celsr3-204* (TB-MO-204), zfl co-injected with TB-MO-204 and human wild-type (wt) *CELSR3* polyA mRNA, zfl injected with scrambled (scrl) CRISPR control and *celsr3* F0 CRISPR knockout (KO) mixes. **a** Representative brightfield microscopy of laterally mounted zfl at two days post fertilization (dpf) treated with 1-phenyl 2-thiourea (PTU). Asterisks: Example caudal end disruption. Arrowhead: Example warped tail. Scale bar 1000 µm. **b** Percentage of affected zfl in brightfield microscopy. TB-MO-204 injected zfl and *celsr3* F0 CRISPR KO zfl show highly significant affection of a warped tail and/or caudal end disruption. In most zfl exposed to TB-MO-204 the phenotype could be rescued with human wt polyA *CELSR3* mRNA. Number (n) of zfl for each injection group: Control-MO ($n = 157$), SB-MO-e6i6 ($n = 278$), TB-MO-204 ($n = 223$), TB-MO-204 + human wt RNA ($n = 221$), scrl CRISPR control ($n = 416$) and *celsr3* F0 CRISPR KO ($n = 440$). Number of independent experiments $N = 3$ for both MO and CRISPR. **c** Representative laterally mounted *Tg(-3.1ngn1:GFP)* zfl at three dpf treated with PTU and imaged from lateral to visualize the effect of Celsr3 MO knockdown (MO-KD) or F0 *celsr3* KO on neurogenesis. The structural irregularities at the caudal end of the MO-KD or F0 *celsr3* KO zfl correlate with a disruption of the neuronal arrangement (white asterisks). Scale bar 1000 µm. **d** Kaplan–Meier plot showing a comparable survival rate for each respective injection group. Number (n) of zf embryos for each injection group: Control-MO ($n = 203$), SB-MO-e6i6 ($n = 367$), TB-MO-204 ($n = 290$), TB-MO-204 + human wt RNA ($n = 272$), scrl CRISPR control ($n = 469$) and *celsr3* F0 CRISPR KO ($n = 611$). Number of independent experiments $N = 3$ each. **e** Representative dorsally mounted *Tg(wt1b:EGFP)* zfl at three dpf treated with PTU and imaged from dorsal to visualize the effect of Celsr3 MO-KD on the development of the pronephros. White asterisk: Example enlarged glomerulus. G: Glomerulus. Ns1: Right neck segment. Ns2: Left neck segment. Scale bar 100 µm. **f** Box plot showing the size of the glomerulus in relation to the neck segments (G/((Ns1 + Ns2)/2)) calculated for each *Tg(wt1b:EGFP)* zfl at three dpf. MO-injected zfl show a highly significant increase of the glomerular diameter in comparison to the length of the neck segments. This effect was almost completely rescued when TB-MO-204 was co-injected together with human *CELSR3* wt polyA mRNA. Control-MO ($n = 22$), TB-MO-204 ($n = 27$), TB-MO-204 + human wt RNA ($n = 29$). Number of independent experiments $N = 3$. *p-value < 0.05, **p-value < 0.01, ***p-value < 0.001, ****p-value < 0.0001, *ns* not significant. Two-way ANOVA. Mean: SEM.

Methods

Ethics declaration

This study fulfilled the requirements of the Declaration of Helsinki and was approved by the Ethics Committee of the Medical Faculty of the University of Bonn (Lfd.Nr.031/19). Consent was obtained for all families including photographs if published, according to the respective research protocol of each institution. Human embryonic and fetal samples were surgically extracted from terminated pregnancies after informed consent and ethics approval. Mouse embryonic tissues have been documented and their usage reported to the local authorities (Regierungspräsidium Darmstadt). Human embryonic tissues were collected after maternal consent and with ethical approval of the North East - Newcastle & North Tyneside 1 Research Ethics Committee (REC18/NE/0290, https://www.hdbr.org). Animal husbandry and experimental setups were in accordance with European Legislation for the Protection of Animals used for Scientific Purposes (Directive 2010/62/EU). National law exempts all zebrafish experiments performed in larval stages up to five dpf before feeding from ethical approval.

Family 1: Written informed consent was obtained from the parents or legal guardians of the study participants after approval from the institutional review board (IRB) at the participating institutions. Approval EK302-16 was granted by the ethics committee of the Medical Faculty of the RWTH Aachen (Universitätsklinikum Aachen, Germany).

Family 2: All individuals or their families have signed written consent including clinical images, approved by the Ethics Committee of the Medical University of Innsbruck. Ethics application number UN4501.

Family 3: All individuals or their families have signed written consent. The study was approved by the IRB protocol 12-009346.

Family 4: All individuals or their families have signed written consent. The individual has been enrolled in a study for sequencing analysis after IRB approval at Policlinico S. Orsola-Malpighi (Bologna, Italy). IRB protocol 3206/2016.

Family 5: All individuals or their families have signed written consent through the Telethon Undiagnosed Disease Program (Naples, Italy).

Family 6: Written consent was obtained for publication of anonymized medical data which were obtained in a diagnostic setting. The affected individual was investigated by their referring physicians and all genetic analyses were performed in a diagnostic setting. Legal guardians of the affected individual gave informed consent for genomic investigations and publication of their anonymized data. For the Erasmus MC, use of genome-wide investigations in a diagnostic setting was IRB approved. IRB protocol METC-2012-387.

Family 7: All individuals or their families have signed written consent. This study was approved by Baylor College of Medicine (Houston, USA). IRB research Protocol H-29697.

Family 8: All individuals or their families have signed written consent through the Telethon Undiagnosed Disease Program (Naples, Italy). This study was approved under protocol number UDP15001. The authors affirm that human research participants provided informed consent for publication of the image in Fig. 1e.

Family 9: All individuals or their families have signed written consent. Agreement to perform Exome Sequencing was obtained by GeneDx (Gaithersburg, USA). Informed consent for publication was obtained from the family by the clinicians and standard permission form to photograph for academic and research purpose was signed.

Family 10: All individuals or their families have signed written consent. Approval for human subjects' research was obtained from the IRB of the University of Michigan and Boston Children's Hospital (Boston, USA). IRB protocol P00006200.

Family 11: All individuals or their families have signed written consent. Approval for human subjects' research was obtained from the IRB of the University of Michigan and Boston Children's Hospital (Boston, USA). IRB protocol P00006200.

Supplementary Family 1: The individual has given written permission for the publication of the data. In Denmark this is not considered a research project and participation is exempt from IRB and ethics approval.

Supplementary Family 2: All individuals or their families have signed written consent. This study was approved by the Columbia University IRB. IRB protocol AAAO6702.

Supplementary Family 3: All individuals or their families have signed written consent including diagnostic and publication.

Variant identification and classification

We describe twelve individuals with bi-allelic variants in *CELSR3*. Furthermore, we describe three families with bi-allelic *CELSR3* variants of uncertain significance in the supplemental material. All individuals were ascertained through clinical exome sequencing (ES) and GeneMatcher[28]. Informed consent was obtained for all cases with additional permission to publish clinical images, if included. Race and ethnicity were self-reported or collected from databases. All sequencing methods, molecular findings and clinical descriptions are stated in Supplement A and B.

All variant alleles refer to the sequence of ENST00000164024.5 (Ensembl release 107, reference sequence NM_001407.3) and were validated with Mutalyzer 2.0.35[29,30]. Due to the size of the gene, we only considered variants not reported homozygous in gnomAD v3.1 and with a gnomAD v3.1 minor allele frequency (MAF) ≤ 0.0001 in order to avoid bi-allelic cases by chance. All variants, and segregation when parents available, were validated by Sanger sequencing. Additional, less likely variants of

unknown significance reported in the here described individuals are mentioned in Supplement A.

For in silico analysis, we used Combined Annotation Dependent Depletion GRCh38-v1.6 (CADD), Polymorphism-Phenotyping v2 (PolyPhen-2) and Sorting Intolerant From Tolerant (SIFT)[31–33]. MetaDome Version 1.0.1 was applied to transcript ENST00000164024.4 to generate a tolerance landscape, analyzing the variants based on the single nucleotide missense and synonymous variants from gnomAD v3.1 in the protein-coding region[34]. Evolutionary conservation of bp positions was estimated using ConSurf[35,36].

Structural modeling of CELSR3 protein and mapping of the variants

PhosphositePlus[16] and AlphaFold[17] were used to model the structure of CELSR3. The source code of the AlphaFold (deepmind) algorithm was downloaded from https://github.com/deepmind/alphafold. Since the human CELSR3 comprising 3,312 aa residues is too large to readily create a full-length model, we split the protein into overlapping subdomains that were individually used as inputs for AlphaFold. The models of the individual domains were structurally aligned using PyMOL. The boundaries of the individual subdomains of the CELSR3 protein with overlapping segments for structural alignment were: 1–240, 121–360, 241–720, 601–840, 721–1320, 1201–1440, 1321–1980, 1861–2100, 1981–2400, 2281–2520, and 2401–3312, respectively.

CELSR3 immunostaining of the human embryonic metanephric kidney and urinary tract

Human embryonic tissues, collected after maternal consent and with ethical approval (REC18/NE/0290), were sourced from the Medical Research Council and Wellcome Trust Human Developmental Biology Resource (https://www.hdbr.org). Samples comprised gestational week 7, 10, and 12. Tissues were paraffin embedded, sectioned as described[37], and immunostained with the following primary antibody: Rabbit polyclonal raised to the N-terminal region of human CELSR3 (1:50 dilution; ab189012 from Abcam). The primary antibody was detected with a secondary antibody (1:200 dilution, Goat Anti-Rabbit ab6720 from Abcam) and signals generated with a DAB (SK-4100) peroxidase-based method[37].

Zebrafish husbandry and embryo maintenance

Zf were maintained according to recommendations by Westerfield[38] and the German national law (animal welfare act and § 11). Zfl of wt AB/TL strain, transgenic *Tg(-3.1ngn1:GFP)* (ZFIN ID: ZDB-TGCONSTRCT-070117-124), and *Tg(wt1b:EGFP)* (ZFIN ID: ZDB-TGCONSTRCT-071127-1) were obtained by natural spawning and raised at 28 °C in Danieau solution on 14 h light and ten hours dark cycle. All experiments were done on zfl at one to five dpf before independent feeding[39].

Morpholino® knockdown and mRNA rescue microinjections

The zf wt ortholog *celsr3* (ENSDARG00000055825) is described with four transcripts (*celsr3-204*: ENSDART00000145095.3; *celsr3-201*: ENSDART00000078334.6; *celsr3-202*: ENSDART00000131888.2; *celsr3-203*: ENSDART00000137391.2; Ensembl release 107)[29]. The sequences of transcript *celsr3-202* and *celsr3-203* in zf are short and completely covered by transcript *celsr3-201*. Furthermore, transcript *celsr3-201* and *celsr3-204* overlap in parts and would be most similar to the only mentioned human transcript *CELSR3-201* as a combined transcript. Hence, analysis of the 5′UTR region with the purpose of identifying an AUG translational start site was performed by extraction of total RNA from 35 zfl with TRIzol™ reagent (Thermo Fisher Scientific, Catalog No. 15596026) and rt-PCR using ProtoScript® II First Strand cDNA Synthesis Kit (New England BioLabs GmbH, Catalog No. E6560). cDNA Amplification of 2138 bp upstream of exon 1 to exon 2 transition of transcript *celsr3-204* was performed using forward primer 5′-GAGCACGGCGGAAGGAGTCG-3′ and reverse primer 5′-CTCTGTAATGATGAGCACCCGCAGC-3′. Celsr3 protein sequence analysis of other species was facilitated using SerialCloner 2.6.1 software. Celsr3 KD was performed using specific Morpholino® Oligonucleotides (MO) synthetized by GeneTools, LLC. Two TB-MOs were designed targeting the AUG translational start site of transcript *celsr3-201* (TB-MO-201, 5′-CTGCTGAGCATCTCCTCTGTAATGA-3′) and the expected AUG translational start site of transcript *celsr3-204* (*celsr3-204* minus 195 bp, TB-MO-204, 5′-GTCTTCTGCAATCACCCACTCCATG-3′). One splice-blocking MO was designed targeting the boundary of *celsr3-204* exon 6 – intron 6 (SB-MO-e6i6, 5′-TCTTCAGTGGACTTTCT-CACCTTGT-3′). In one- to two-cell zf embryos, MO microinjections were performed into the yolk with *celsr3* TB-MO-201, *celsr3* TB-MO-204 or the standard control MO (Control-MO, 5′-CCTCTTACCTCAGTTA-CAATTTATA-3′) with ~4.5 ng for each MO (1.8 nl/embryo), or with ~5.9 ng for *celsr3* SB-MO-e6i6 (1.8 nl/embryo). For mRNA rescue experiments, ~70 pg of in vitro transcribed human wt *CELSR3* polyA mRNA and TB-MO-204 with non-identical sequences (bp) were co-injected. mRNA transcription was performed on human *CELSR3* cDNA ORF clone OHu18524 (GenScript) containing NM_001407.3 using the mMESSAGE mMACHINE T7 Ultra Kit (Thermo Fisher Scientific, Catalog No. AMB13455) followed by polyA tailing using Invitrogen™ Poly-(A) Tailing Kit (ThermoFisher, Invitrogen™, Catalog No. AM1350). For zfl injection, concentrations were chosen to avoid dose-dependent effects after examination ranges of ~3.7–7.4 ng MO and 20–100 pg/nl mRNA solution.

CRISPR–Cas9 F0 knockout of *celsr3*

F0 KO zfl were generated using the CRISPR-Cas9 method as previously described with slight modifications to the protocol[40]. With the purpose of creating a truncated *celsr3* transcript we designed six sgRNAs binding shortly upstream of exon 1, in exon 1 and in exon 2 of *celsr3-204* (NM_001407.3) using the open website tool https://www.crisprscan.org/[41]. Reagents of Alt-R™ CRISPR-Cas9 System (Alt-R® CRISPR-Cas9 crRNA, custom design; Alt-R® CRISPR-Cas9 tracrRNA; Alt-R® S.p. Cas9 Nuclease V3, Catalog No. 1081058; Alt-R® CRISPR-Cas9 Negative "scrambled" control crRNA #1-#3, Catalog No. 1072544-1072546; Nuclease-Free Duplex Buffer, Catalog No. 11-05-01-12) were obtained from Integrated DNA Technologies, Inc and prepared according to the distributor's and user protocols[42]. Equal amounts of either all six *celsr3* sgRNAs or the three scrambled control sgRNAs were combined to a 100 µM stock. Equal amounts of these 100 µM sgRNA stocks and 100 µM tracrRNA were diluted in Nuclease-Free Duplex Buffer to a final concentration of 3 µM or 6 µM for scrambled control and *celsr3* mix and annealed at 95 °C for 5 min. These were combined with the same amount (3.05/6.1 µM) of Cas9 protein diluted in Cas9 working buffer each and incubated at 37 °C for 10 min. Shortly before injections 1 µl of phenol red was added. Injections of ~1.8 nl were performed into the yolk of one- to two-cell zf embryos. Truncation of the *celsr3* genomic region was PCR tested at four dpf as previously described[43]. Primer sequences, sgRNA sequences and genomic PCR-gel electrophoresis images are provided in Supplementary Fig. 4.

In vivo imaging and phenotyping

Zf embryos were incubated with 0.2 mM 1-phenyl 2-thiourea (PTU, Catalog No. P7629) supplemented to their Danieau solution from one to five dpf to avoid pigmentation. Brightfield and fluorescence in vivo imaging was performed from one to five dpf using a ZEISS Axio V16 Multi-Zoom microscope and analyzed with ZEN 2.3 Software. Phenotypic affection in brightfield imaging was defined by the presence of irregular tail curvature and/or disruption at the caudal end at two dpf. For CNS phenotype evaluation *Tg(-3.1ngn1:GFP)* zfl at three dpf were anesthetized with 0.03% tricaine and fixed in 1.25% low-melting agarose. For evaluation of the urinary tract phenotype *Tg(wt1b:EGFP)* zfl at three dpf were anesthetized and fixed as described above. Z-stack-series with 2 µm step size was performed with a Nikon A1R HD25 ECLIPSE Ti2E confocal laser scanning microscope equipped with NIS-Elements 5.21.02 software. Phenotypic differences in the developing pronephros in *Tg(wt1b:EGFP)* were analyzed with the NIS-Element imaging software 5.21.00. To account for variation in larvae size, the glomerulus diameter was normalized to the respective length

of the pronephric neck segments. All experiments were repeated independently at least three times ($N \geq 3$).

Statistical analyses

GraphPad Prism Version 9.0.0 was used for one-way ANOVA with post-hoc Tukey HSD Test and two-way ANOVA with SEM. Kaplan–Meier survival curves were used to analyze survival within the first five dpf.

Reporting summary

Further information on research design is available in the Nature Research Reporting Summary linked to this article.

Data availability

Data supporting the findings of this study are available in the supplemental material. Additional data not compromised by ethical issues will be available upon request from the corresponding authors. All sequencing data are deposited in ClinVar (accession numbers: SCV004176841 – SCV004176856). Mouse RNA-seq data at stages E10.5, E12.5 and E15.5 were obtained from Gene Expression Omnibus (GEO accession ID: GSE190641)[23]. RNA-seq data of human embryonic and fetal bladder tissues were obtained from already deposited data at EMBL-EBI expression atlas (E-MTAB-6592).

Received: 16 August 2023; Accepted: 26 January 2024;
Published online: 01 March 2024

References

1. Colin, E. et al. Loss-of-function mutations in WDR73 are responsible for microcephaly and steroid-resistant nephrotic syndrome: Galloway-Mowat syndrome. *Am. J. Hum. Genet.* **95**, 637–648 (2014).
2. Heidet, L. et al. Targeted Exome Sequencing Identifies PBX1 as Involved in Monogenic Congenital Anomalies of the Kidney and Urinary Tract. *J. Am. Soc. Nephrol. JASN* **28**, 2901–2914 (2017).
3. Connaughton, D. M. et al. Mutations of the Transcriptional Corepressor ZMYM2 Cause Syndromic Urinary Tract Malformations. *Am. J. Hum. Genet.* **107**, 727–742 (2020).
4. Wang, X.-J. et al. Understanding cadherin EGF LAG seven-pass G-type receptors. *J. Neurochem.* **131**, 699–711 (2014).
5. Goffinet, A. M. & Tissir, F. Seven pass Cadherins CELSR1-3. *Semin. Cell Dev. Biol.* **69**, 102–110 (2017).
6. Brzóska, H. Ł. et al. Planar cell polarity genes Celsr1 and Vangl2 are necessary for kidney growth, differentiation, and rostrocaudal patterning. *Kidney Int.* **90**, 1274–1284 (2016).
7. Zhang, B., Tran, U. & Wessely, O. Expression of Wnt signaling components during Xenopus pronephros development. *PloS One* **6**, e26533 (2011).
8. Shima, Y. et al. Differential expression of the seven-pass transmembrane cadherin genes Celsr1-3 and distribution of the Celsr2 protein during mouse development. *Dev. Dyn.* **223**, 321–332 (2002).
9. Tissir, F., Bar, I., Jossin, Y., de Backer, O. & Goffinet, A. M. Protocadherin Celsr3 is crucial in axonal tract development. *Nat. Neurosci.* **8**, 451–457 (2005).
10. Zhou, L. et al. Early forebrain wiring: genetic dissection using conditional Celsr3 mutant mice. *Science* **320**, 946–949 (2008).
11. Chen, B. et al. Celsr3 Inactivation in the Brainstem Impairs Rubrospinal Tract Development and Mouse Behaviors in Motor Coordination and Mechanic-Induced Response. *Mol. Neurobiol.* **59**, 5179–5192 (2022).
12. Chen, Z. et al. Genetic analysis of Wnt/PCP genes in neural tube defects. *BMC Med. Genom.* **11**, 38 (2018).
13. Li, J. et al. CELSR3 variants are associated with febrile seizures and epilepsy with antecedent febrile seizures. *CNS Neurosci. Therapeutics* **28**, 382–389 (2022).
14. Wang, S. et al. De Novo Sequence and Copy Number Variants Are Strongly Associated with Tourette Disorder and Implicate Cell Polarity in Pathogenesis. *Cell Rep.* **25**, 3544 (2018).
15. Reutter, H. et al. Genetics of Bladder-Exstrophy-Epispadias Complex (BEEC): Systematic Elucidation of Mendelian and Multifactorial Phenotypes. *Curr. Genomics* **17**, 4–13 (2016).
16. Hornbeck, P. V. et al. PhosphoSitePlus, 2014: mutations, PTMs and recalibrations. *Nucleic Acids Res.* **43**, D512–D520 (2015).
17. Jumper, J. et al. Highly accurate protein structure prediction with AlphaFold. *Nature* **596**, 583–589 (2021).
18. Araç, D. et al. A novel evolutionarily conserved domain of cell-adhesion GPCRs mediates autoproteolysis. *EMBO J.* **31**, 1364–1378 (2012).
19. Okamoto, Y., Bernstein, J. D. & Shikano, S. Role of C-terminal membrane-proximal basic residues in cell surface trafficking of HIV coreceptor GPR15 protein. *J. Biol. Chem.* **288**, 9189–9199 (2013).
20. Nishimura, T., Honda, H. & Takeichi, M. Planar cell polarity links axes of spatial dynamics in neural-tube closure. *Cell* **149**, 1084–1097 (2012).
21. Allache, R. et al. Role of the planar cell polarity gene CELSR1 in neural tube defects and caudal agenesis. *Birth Defects Res. Part A Clin. Mol. Teratol.* **94**, 176–181 (2012).
22. Wang, L. et al. Digenic variants of planar cell polarity genes in human neural tube defect patients. *Mol. Genet. Metab.* **124**, 94–100 (2018).
23. Mingardo, E. et al. A genome-wide association study with tissue transcriptomics identifies genetic drivers for classic bladder exstrophy. *Commun. Biol.* **5**, 1203 (2022).
24. Harty, B. L., Krishnan, A., Sanchez, N. E., Schiöth, H. B. & Monk, K. R. Defining the gene repertoire and spatiotemporal expression profiles of adhesion G protein-coupled receptors in zebrafish. *BMC Genom.* **16**, 62 (2015).
25. Drabkin, H. J. & RajBhandary, U. L. Initiation of protein synthesis in mammalian cells with codons other than AUG and amino acids other than methionine. *Mol. Cell. Biol.* **18**, 5140–5147 (1998).
26. Joshi, B., Gaur, H., Hui, S. P. & Patra, C. Celsr family genes are dynamically expressed in embryonic and juvenile zebrafish. *Dev. Neurobiol.* **82**, 192–213 (2022).
27. Rieke, J. M. et al. SLC20A1 Is Involved in Urinary Tract and Urorectal Development. *Front. Cell Dev. Biol.* **8**, 567 (2020).
28. Sobreira, N., Schiettecatte, F., Valle, D. & Hamosh, A. GeneMatcher: a matching tool for connecting investigators with an interest in the same gene. *Hum. Mutat.* **36**, 928–930 (2015).
29. Cunningham, F. et al. Ensembl 2022. *Nucleic Acids Res.* **50**, D988–D995 (2022).
30. Lefter, M. et al. Mutalyzer 2: next generation HGVS nomenclature checker. *Bioinformatics* **37**, 2811–2817 (2021).
31. Rentzsch, P., Witten, D., Cooper, G. M., Shendure, J. & Kircher, M. CADD: predicting the deleteriousness of variants throughout the human genome. *Nucleic Acids Res.* **47**, D886–D894 (2019).
32. Adzhubei, I. A. et al. A method and server for predicting damaging missense mutations. *Nat. Methods* **7**, 248–249 (2010).
33. Sim, N.-L. et al. SIFT web server: predicting effects of amino acid substitutions on proteins. *Nucleic Acids Res.* **40**, W452–W457 (2012).
34. Wiel, L. et al. MetaDome: Pathogenicity analysis of genetic variants through aggregation of homologous human protein domains. *Hum. Mutat.* **40**, 1030–1038 (2019).
35. Ben Chorin, A. et al. ConSurf-DB: An accessible repository for the evolutionary conservation patterns of the majority of PDB proteins. *Protein Sci.* **29**, 258–267 (2020).
36. Goldenberg, O., Erez, E., Nimrod, G. & Ben-Tal, N. The ConSurf-DB: pre-calculated evolutionary conservation profiles of protein structures. *Nucleic Acids Res.* **37**, D323–D327 (2009).
37. Lopes, F. M., Roberts, N. A., Zeef, L. A., Gardiner, N. J. & Woolf, A. S. Overactivity or blockade of transforming growth factor-β each

generate a specific ureter malformation. *J. Pathol.* **249**, 472–484 (2019).
38. Westerfield M. *The Zebrafish Book: A Guide for the Laboratory Use of Zebrafish* (University of Oregon Press, 2007).
39. Dworschak, G. C. et al. Biallelic and monoallelic variants in PLXNA1 are implicated in a novel neurodevelopmental disorder with variable cerebral and eye anomalies. *Genet. Med.* **23**, 1715–1725 (2021).
40. Kroll, F. et al. A simple and effective F0 knockout method for rapid screening of behaviour and other complex phenotypes. eLife **10**, e59683 (2021).
41. Moreno-Mateos, M. A. et al. CRISPRscan: designing highly efficient sgRNAs for CRISPR-Cas9 targeting in vivo. *Nat. Methods* **12**, 982–988 (2015).
42. Essner J. Zebrafish embryo microinjection Ribonucleoprotein delivery using the Alt-RTM CRISPR-Cas9 System. User Methods, IDT Inc. Coralville, IA, Integrated DNA Technologies. https://idtdevblob.blob.core.windows.net/sitefinity/docs/default-source/user-submitted-method/crispr-cas9-rnp-delivery-zebrafish-embryos-j-essnerc46b5a1532796e2eaa53ff00001c1b3c.pdf?sfvrsn=52123407_10 (2016).
43. Meeker, N. D., Hutchinson, S. A., Ho, L. & Trede, N. S. Method for isolation of PCR-ready genomic DNA from zebrafish tissues. *BioTechniques* **43**, 610, 612, 614 (2007).

Acknowledgements

We thank all individuals and their families for their contribution to this study. J.D.S. is supported by BonnNI grant Q614.2454 and supervised by H.R. J.C.K. is supported by BonnNi grant Q614.0754 and BONFOR grant O-167.0023. G.C.D. is supported by BONFOR grant O-120.0001 and the Herbert-Reeck foundation (2019). Further we thank the Zebrafish Core Facility (Bonn Medical Faculty) for support. *Tg(wt1b:EGFP)* zf were provided by Prof. Christoph Englert (Leibniz-Institut, Jena) and *Tg(-3.1ngn1:GFP)* by the European Zebrafish Resource Centre (EZRC, Karlsruhe). This work was further supported in part by the US National Institutes of Health, National Institute of Neurologic Disease and Stroke [R35 NS105078] and the Muscular Dystrophy Association [#512848] to J.R.L; and National Human Genome Research Institute (NHGRI) program grants [UM1 HG006542; U01 HG011758]. J.E.P. was supported by the National Institutes of Health NHGRI [K08 HG008986]. A.S.W. and F.M.L. acknowledge grant support from the Medical Research Council (project grant MR/T016809/1). A.S.W. acknowledges support from the MCR-NIHR UK Rare Disease Research Platform Rare early onset lower urinary tract (REOLUT) disorders MR/Y008340/1 and project start-up research funding from Kidneys for Life. This work was supported in part by Telethon Undiagnosed Diseases Program (TUDP, GSP15001). I.V. is supported by grant by the Novo Nordic Foundation Grant no NNF16OC0018772. F.H. is the William E. Harmon Professor of Pediatrics at Harvard Medical School. This research was supported by grants from the National Institutes of Health to F.H. (DK076683). Sequencing and data processing was partly performed by the Yale Centers for Mendelian Genomics funded by the National Human Genome Research Institute (U54 HG006504). Data analysis was partly performed by Jill A Rosenfeld, Baylor College of Medicine and Baylor Genetics Laboratories, Houston, TX 77030, USA. S.Se. is supported by the German Research Foundation (Deutsche Forschungsgemeinschaft, DFG; 442070894). F.H. and S.Sh. are supported by grants from the Begg Family Foundation. V.C. would like to acknowledge ERN ITHACA that improve clinical practice within EU. The Barakat lab was supported by the Netherlands Organisation for Scientific Research (ZonMW Veni, grant 91617021), an Erasmus MC Fellowship 2017, and Erasmus MC Human Disease Model Award 2018. H.R. is supported by the German Research Foundation (Deutsche Forschungsgemeinschaft, DFG, RE 1723/5-1). This research was also supported by the Isabella Forrest Julian Research Fund for Pediatric Post Kidney Transplant Research. A.C.H. was partially funded by the Else Kröner-Fresenius-Stiftung and the Eva Luise und Horst Köhler Stiftung – Project No: 2019_KollegSE.04, and further by the the Interdisciplinary Center for Clinical Research (IZKF) at the University Hospital of the Friedrich-Alexander-Universität (FAU) (project J98 and CSP). We acknowledge financial support by Deutsche Forschungsgemeinschaft and Friedrich-Alexander-Universität Erlangen-Nürnberg within the funding program "Open Access Publication Funding". This work was supported by the Open Access Publication Fund of the University of Bonn.

Author contributions

Conceptualization: J.D.S., J.C.K., G.C.D., H.R., G.H., M.G., B.O., A.C.H.; Data curation: J.D.S., J.C.K., P.G., E.M., F.M.L., H.R.; Formal analysis: J.D.S., N.I., E.M., F.M.L., G.H.; Investigation: J.D.S., J.C.K., G.C.D., N.I., E.M., F.M.L., Y.M.H., P.G., T.T.L., Ö.Y., K.C., S.Se., S.Sh., F.H., F.B., A.H., A.J., K.My., K.Mc., M.R.B., N.B., M.S., M.M., V.N., A.T., M.P., V.C., A.A., S.M., A.Sp., R.J.O., E.W.K., B.C.L., S.S.J., J.C., P.S., D.R., A.R.J., J.V., I.V., J.B.F., J.L.C., K.R., V.K., L.E.W., M.Be., M.E., T.E., A.St., K.S., M.V.S., T.S.B., M.S.M., T.T.S., C.C., R.W., F.I., T.P., G.S., F.M., M.C.K., S.B., H.D., H.R., G.H., M.G., A.S.W., J.E.P., J.R.L., B.O., A.C.H.; Methodology: J.D.S., G.H., A.S.W., B.O., A.C.H.; Resources: H.R., M.G., A.S.W., J.R.L., B.O.; Visualization: J.D.S., F.M.L., G.H.; Writing - original draft: J.D.S., J.C.K., N.I., H.R., A.S.W, B.O., A.C.H.; Writing - review & editing: J.D.S., J.C.K., B.O., A.C.H.; First authors J.D.S. and J.C.K. as well as last authors B.O. and A.C.H. contributed equally to this work.

Funding

Open Access funding enabled and organized by Projekt DEAL.

Competing interests

The Department of Molecular & Human Genetics at Baylor College of Medicine receives revenue from clinical genetic testing completed at Baylor Genetics (BG) Laboratories. J.R.L. serves on the Scientific Advisory Board of BG. J.R.L. has stock ownership in 23andMe and is a co-inventor on multiple United States and European patents related to molecular diagnostics for inherited neuropathies, eye diseases, genomic disorders, and bacterial genomic fingerprinting. The other authors declare no competing interests.

Additional information

Supplementary information The online version contains supplementary material available at https://doi.org/10.1038/s41525-024-00398-9.

Correspondence and requests for materials should be addressed to Jil D. Stegmann or Alina C. Hilger.

Reprints and permissions information is available at http://www.nature.com/reprints

Publisher's note Springer Nature remains neutral with regard to jurisdictional claims in published maps and institutional affiliations.

Open Access This article is licensed under a Creative Commons Attribution 4.0 International License, which permits use, sharing, adaptation, distribution and reproduction in any medium or format, as long as you give appropriate credit to the original author(s) and the source, provide a link to the Creative Commons licence, and indicate if changes were made. The images or other third party material in this article are included in the article's Creative Commons licence, unless indicated otherwise in a credit line to the material. If material is not included in the article's Creative Commons licence and your intended use is not permitted by statutory regulation or exceeds the permitted use, you will need to obtain permission directly from the copyright holder. To view a copy of this licence, visit http://creativecommons.org/licenses/by/4.0/.

© The Author(s) 2024

[1]Institute of Human Genetics, Medical Faculty, University of Bonn, Bonn 53127, Germany. [2]Institute of Anatomy and Cell Biology, Medical Faculty, University of Bonn, Bonn 53115, Germany. [3]Institute of Neuroanatomy, Medical Faculty, University of Bonn, Bonn 53115, Germany. [4]Department of Neuropediatrics, University Hospital Bonn, Bonn 53127, Germany. [5]Division of Cell Matrix Biology and Regenerative Medicine, School of Biological Sciences, Faculty of Biology Medicine and Health, University of Manchester, Manchester, UK. [6]Georg-Speyer-Haus, Institute for Tumor Biology and Experimental Therapy, 60596 Frankfurt am Main, Germany. [7]Division of Nephrology, Department of Pediatrics, Boston Children's Hospital, Harvard Medical School, Boston, MA, USA. [8]Institute of Medical Genetics and Human Genetics, Charité Universitätsmedizin Berlin, corporate member of Freie Universität Berlin and Humboldt-Universität zu Berlin, Berlin, Germany. [9]Department of Pediatrics, Medizinische Fakultät Carl Gustav Carus, Technische Universität Dresden, Dresden, Germany. [10]Department of Molecular & Human Genetics, Baylor College of Medicine, Houston, TX 77030, USA. [11]Medical Scientist Training Program, Baylor College of Medicine, Houston, TX, USA. [12]Center for Cardiovascular Research, Nationwide Children's Hospital, Department of Pediatrics, Ohio State University, Columbus, OH, USA. [13]Department of Pediatrics, Renal Service, Texas Children's Hospital, Houston, TX 77030, USA. [14]Department of Pediatrics, Baylor College of Medicine, Houston, TX 77030, USA. [15]Department of Neurosciences, Rehabilitation, Ophthalmology, Genetics, Maternal and Child Health (DINOGMI), University of Genoa, 16132 Genoa, Italy. [16] U.O.C. Genetica Medica, IRCCS Istituto Giannina Gaslini, 16147 Genoa, Italy. [17]Medical Genetics, Department of Precision Medicine, Università degli Studi della Campania 'Luigi Vanvitelli', via Luigi De Crecchio 7, 80138 Naples, Italy. [18]Telethon Institute of Genetics and Medicine, Pozzuoli, Naples, Italy. [19]Department of Molecular Medicine and Medical Biotechnologies, University Federico II, Naples, Italy. [20]Genomics and Clinical Genetics, IRCCS Gaslini, Genoa, Italy. [21]Division of Medical Genetics, Department of Specialized Medicine, McGill University, Montreal, QC, Canada. [22]Department of Human Genetics, McGill University, Montreal, QC, Canada. [23] Medical Genetics Service, Oncology Department of Southern Switzerland, Ente Ospedaliero Cantonale, Lugano, Switzerland. [24]MBBM Foundation, Monza, Italy. [25]Center for Individualized Medicine, Mayo Clinic, Rochester, MN, USA. [26]Department of Clinical Genomics, Mayo Clinic, Rochester, MN, USA. [27]Department of Quantitative Health Sciences, Mayo Clinic, Rochester, MN, USA. [28]Department of Pediatrics, Seoul National University College of Medicine, Seoul, Republic of Korea. [29]Department of Genomics Medicine, Rare Disease Center, Seoul National University Hospital, Seoul, Republic of Korea. [30]Division of Neonatology, Pediatric Intensive Care and Neuropediatrics, Comprehensive Center for Pediatrics, Medical University of Vienna, Vienna, Austria. [31]Division of Bioinformatics, Medical University of Innsbruck, 6020 Innsbruck, Austria. [32]Department of Pediatrics I, Medical University of Innsbruck, 6020 Innsbruck, Austria. [33]Division of Human Genetics, Medical University of Innsbruck, 6020 Innsbruck, Austria. [34]Department of Pediatrics and Adolescent Medicine, Division of Pediatric Pulmonology, Allergology and Endocrinology, Comprehensive Center for Pediatrics, Medical University of Vienna, 1090 Vienna, Austria. [35]Department of Clinical Medicine, Aarhus University, Aarhus, Denmark. [36]Department of Clinical Genetics, Aarhus University Hospital, Aarhus, Denmark. [37]Division of Medical Genetics, Department of Pediatrics, Duke University, Durham, NC, USA. [38]Department of Pediatrics, Duke University Medical Center, Durham, NC, USA. [39]Pediatric Neurology, Riley Hospital for Children Indiana University Health, Indianapolis, IN, USA. [40]Institute for Human Genetics and Genomic Medicine, Medical Faculty, RWTH Aachen University, Aachen, Germany. [41]Division of Neuropediatrics and Social Pediatrics, Department of Pediatrics, Medical Faculty, RWTH Aachen University, 52074 Aachen, Germany. [42]Department of Clinical Genetics, Erasmus MC University Medical Center, Rotterdam, The Netherlands. [43]Department of Neurology, Columbia University Vagelos College of Physicians and Surgeons, New York, NY, USA. [44]Department of Pathology, Columbia University Vagelos College of Physicians and Surgeons, New York, NY, USA. [45]Division of Child Neurology, Department of Neurology, Columbia University Vagelos College of Physicians and Surgeons and NewYork-Presbyterian Morgan Stanley Children's Hospital, New York, NY, USA. [46]Department of Pediatrics, Columbia University Vagelos College of Physicians and Surgeons and NewYork-Presbyterian Morgan Stanley Children's Hospital, New York, NY, USA. [47]Institute for Genomic Medicine, Columbia University Vagelos College of Physicians and Surgeons, New York, NY, USA. [48]Department of Genetic Counselling, The Hospital for Sick Children, Toronto, ON M5G 1X8, Canada. [49]Department of Molecular Genetics, University of Toronto, Toronto, ON M5S 1A1, Canada. [50]Division of Clinical and Metabolic Genetics, The Hospital for Sick Children, Toronto, ON M5G 1X8, Canada. [51]U.O. Genetica Medica, IRCCS Azienda Ospedaliero-Universitaria di Bologna, Bologna, Italy. [52]Pediatric Movement Disorders Program, Division of Pediatric Neurology, Barrow Neurological Institute, Phoenix Children's Hospital, Phoenix, AZ, USA. [53]Departments of Child Health, Neurology, and Cellular & Molecular Medicine, and Program in Genetics, University of Arizona College of Medicine–Phoenix, Phoenix, AZ, USA. [54]Neuroscience Research Center, Faculty of Medicine, Golestan University of Medical Sciences, Gorgan, Iran. [55]Division Neonatology and Pediatric Intensive Care, Department of Pediatric and Adolescent Medicine, Friedrich-Alexander University of Erlangen-Nürnberg, Erlangen, Germany. [56]Institute of Human Genetics, Friedrich-Alexander University of Erlangen-Nürnberg, Erlangen, Germany. [57]Institute of Structural Biology, University Hospital Bonn, University of Bonn, Venusberg-Campus 1, 53127 Bonn, Germany. [58]Royal Manchester Children's Hospital, Manchester University NHS Foundation Trust, Manchester Academic Health Science Centre, Manchester, UK. [59]Human Genome Sequencing Center, Baylor College of Medicine, Houston, TX 77030, USA. [60]Texas Children's Hospital, Houston, TX 77030, USA. [61]Department of Pediatric and Adolescent Medicine, Friedrich-Alexander University of Erlangen-Nürnberg, Erlangen 91054, Germany. [62]Research Center On Rare Kidney Diseases (RECORD), University Hospital Erlangen, 91054 Erlangen, Germany. [63]These authors contributed equally: Jil D. Stegmann, Jeshurun C. Kalanithy [64]These authors jointly supervised this work: Benjamin Odermatt, Alina C. Hilger. *A list of authors and their affiliations appears at the end of the paper.
✉e-mail: jil.stegmann@uni-bonn.de; alina.hilger@uk-erlangen.de

TUDP consortium

Manuela Morleo[17,18], Vincenzo Nigro[17,18] & Annalaura Torella[17,18]

3. Danksagung

An erster Stelle möchte ich mich herzlich bei meinem Doktorvater Prof. Dr. Heiko Reutter bedanken. In allen Phasen dieser Dissertation hat er mich hervorragend betreut und sowohl fachlich als auch organisatorisch zu jedem Zeitpunkt unterstützt.

Ich möchte mich außerdem herzlich bei Prof. Dr. Benjamin Odermatt bedanken, der die Experimente im Zebrafisch ermöglicht hat und mir jederzeit bei allen Fragen zur Seite stand.

Der gesamten Arbeitsgruppe in der Humangenetik und dem Anatomischen Institut danke ich sehr für die große Unterstützung in den letzten Jahren und der schönen gemeinsamen Zeit. Dabei bedanke ich mich besonders bei Jeshurun Kalanithy, Dr. Alina Hilger, Selina Hölzel, Dr. Enrico Mingardo, Paulina Kempe, Lea Waffenschmidt, Ricarda Köllges, Sophia Schneider, Julia Fabian, Clara Vidic, Corina Thiem, Dr. Gabriel Dworschak, Dr. Nina Ishorst, Tobias Lindenberg, Öznur Yilmaz, Khadija Channab und Julia Fazaal.

Dem Bonner Promotionskolleg "NeuroImmunology" (BonnNi) danke ich für die finanzielle Unterstützung dieser Dissertation.

Ich danke der Zebrafish Core Facility und der Next Generation Sequencing Core Facility der Medizinischen Fakultät der Universität Bonn für die Ermöglichung der experimentellen Studien.

Außerdem danke ich allen Patientinnen und Patienten und deren Familien, die an unseren Studien teilgenommen haben.

Mein herzlicher Dank gilt Nicolai Mertens und all meinen Freundinnen und Freunden für die vielfältige Unterstützung in den letzten Jahren.

Zuletzt möchte ich mich von ganzem Herzen bei meinen Eltern Ursula und Wolfgang, sowie meinen Schwestern Kim und Lea bedanken, für die umfangreiche Unterstützung während der Dissertation, des gesamten Studiums und darüber hinaus.